CHALMERS
UNIVERSITY OF TECHNOLOGY

PLA Compounds for Manufacturing of Fossil-free Filaments for 3D Printing

Master's thesis in Materials Chemistry

Linnea Jonsson

Department of Industrial and Materials Science
CHALMERS UNIVERSITY OF TECHNOLOGY
Gothenburg, Sweden 2019

Master's thesis 2019

PLA Compounds for Manufacturing of Fossil-free Filaments for 3D Printing

LINNEA JONSSON

CHALMERS
UNIVERSITY OF TECHNOLOGY

Department of Industrial and Materials Science
Division of Engineering Materials
Chalmers University of Technology
Gothenburg, Sweden 2019

PLA Compounds for Manufacturing of Fossil-free Filaments for 3D Printing
LINNEA JONSSON

Supervisors: Camilla Johansson and Ali Moyassari, Chalmers Industriteknik,
Abhijit Venkatesh, Department of Industrial and Materials Science
Examiner: Antal Boldizar, Department of Industrial and Materials Science

Master's Thesis 2019
Department of Industrial and Materials Science
Division of Engineering Materials
Chalmers University of Technology
SE-412 96 Gothenburg
Telephone +46 31 772 1000

Cover: The raw material used and the pellets and the test specimens produced within the project.

Gothenburg, Sweden 2019

PLA Compounds for Manufacturing of Fossil-free Filaments for 3D Printing
LINNEA JONSSON
Department of Industrial and Materials Science
Chalmers University of Technology

Abstract

The two polymers most widely used in 3D printing are acrylonitrile butadiene styrene (ABS) and polylacic acid (PLA). It is of great importance to reduce the use of the fossil-based ABS by substituting it with a material with less environmental impact, such as the bio-based PLA. The brittleness of PLA is however a drawback that limits the use of the material.

The aim of this master's thesis is to obtain PLA-based compounds, suitable for 3D printing, with enhanced properties which makes it possible to replace, at least to some extent, fossil-based filaments.

From evaluating the state of the art it was concluded that thermoplastic poyurethane (TPU) and acetyl tributyl citrate (ATBC) are additives that can reduce the brittleness of PLA. Five different compounds (PLA, PLA+2%ATBC, PLA+2%TPU, PLA+5%TPU and PLA+12%TPU) were produced by extrusion and their properties were characterized using DSC, capillary viscometry, impact test and tensile test.

All compounds showed transition temperatures similar to pure PLA and suitable viscosity at the shear rates used in 3D printing. With respect to the transition temperatures of the compounds and their viscosity, all the compounds are potentially suitable filaments for 3D printing.

The addition of 2% ATBC and 2% TPU did not improve the impact strength or the properties obtained from the tensile test significantly. The impact strength was improved by the addition of 5% and 12% TPU and the tensile test showed that these compounds increased the elongation at break and decreased Young's modulus, which indicates that these compounds are more ductile than pure PLA. It can therefore be concluded that PLA+5%TPU and PLA+12%TPU are the compounds investigated in this project that could be suitable to use as 3D printing filaments. Additional investigations, in particular of the morphology and miscibility of the compounds, are however necessary to verify the results and to further understand the properties of the compounds.

Keywords: Polylactic acid (PLA), bio-based compounds, thermoplastic polyurethane (TPU), acetyl tributyl citrate (ATBC), 3D printing, FDM.

Acknowledgements

I would like to thank my supervisors at Chalmers Industriteknik, Camilla Johansson and Ali Moyassari, for their valuable guidance and feedback. I would also like to thank Abhijit Venkatesh and Lilian Forsgren for their help and support with the experimental work of the project, and Ida Östergren for sharing her knowledge and experience in 3D printing. Lastly, I would like to thank my examiner Antal Boldizar for his commitment throughout the project.

Linnea Jonsson, Gothenburg, May 2019

Contents

1
Introduction

The increasing environmental concern makes the replacement of fossil-based materials to bio-based substitutes almost inevitable. It is well known that plastic materials have a high environmental impact since many polymers are produced from raw material originating from the petrochemical industry[1]. Plastics can in some cases contribute to a more sustainable society, for example due to their light weight[1], but readjustment towards an increasing use of bio-based materials is nevertheless important.

A field where polymeric materials are used to a great extent is fused deposition modeling (FDM)[2]. This is a type of 3D printing technique which by layer-wise deposition produces a printed object based on a computerized design[2]. Due to their low melting point, thermoplastics are often used in FDM[2] and acrylonitrile butadiene styrene (ABS) and polylactic acid (PLA) are the two polymers most widely used[3]. ABS is a fossil-based polymer and its production has the largest environmental impact in respect to CO_2 emissions when compared to other fossil-based commercial plastics[1]. It is therefore of great importance to reduce the use of ABS in the 3D printing field by substituting it with a material with less environmental impact, such as PLA.

PLA is a bio-based polymer that overall has good mechanical properties and shows promising printing properties, such as less warping compared to ABS, but its inherent brittleness is the main drawback which limits the use of the material[4]. Today, PLA is mainly produced from corn starch or sugarcane[5]. This gives rise to a debate whether crops, and by extension, food, should be used for industrial production of materials. Corn is mostly cultivated in the United States[6] while sugarcane grows in tropical and subtropical areas of the world[7]. This can be seen as an incitement to introduce a more local production of PLA in Europe. Producing PLA from the Swedish forest would not only limit the current transport of raw materials around the world, but it would also be a solution to the food debate. Furthermore, if it is possible to produce PLA from the forest industry waste, the production would not compete with the existing pulp and paper industry and material that otherwise would be combusted could be used more efficiently.

This master's thesis is a part of a Vinnova financed project led by Add North (producer of 3D print filaments) which aims to produce PLA from the Swedish forest. In addition, the project led by Add North aims to find ways to modify PLA filaments in such a way that they, at least to some extent, can replace fossil-based filaments. This part of the project is led by Chalmers Industriteknik.

1.1 Aim

The aim of this master's thesis is to obtain PLA-based compounds, suitable for 3D printing, with enhanced properties which makes it possible to replace, at least to some extent, fossil-based filaments.

1.2 Limitations

To obtain enhanced properties of PLA, modification can be done by blending PLA with a range of different additives, and both bio-based and fossil-based additives have shown to be successful in modifying the mechanical and thermal properties of PLA[4, 8]. However, since the long-term goal is to replace fossil-based materials with bio-based substitutes, the project is limited to compounding PLA (NatureWorks Inego^{TM} Biopolymer 4043D) with bio-based additives to produce a filament that is completely bio-based. The potential fossil-based additives are therefore only considered in the initial literature study to gain knowledge of the state of the art, but are not included in the experimental investigation.

It is possible to investigate not only bio-based additives but also those that in addition are biodegradable. Since PLA is biodegradable[4], compounding it with another biodegradable material opens up for a wider area of application. The same line of reasoning can be applied on the biocompatibility, making the filament potentially suitable for printable medical devices such as implants. The strive towards a broader usage of the filament can however decrease the number of potential additives, which might become a hindrance in the project. These latter parameters are therefore not prioritized, but nevertheless welcomed if achieved.

In addition to being bio-based, the additives used must also be economically tenable, since it will be difficult to commercialize the produced filaments if they in the end are very expensive. The idea, to further enhance the commercialization of the filament, is that the additives already should exist as commercial products, where no chemical modifications should be needed before producing the compounds. The aim is therefore to use only additives that in their original form are possible to mechanically blend with PLA.

Another economical aspect that is important to examine is the filament production. It must be economically viable to extract the PLA from the raw wood material and to produce the compounded filament in order to ensure a potential market. This

aspect is not included in this project. Instead, the material properties, the thermal and mechanical properties in particular, of such a compound is the main focus.

1.3 Specification of issue under investigation

To outrival the fossil-based filaments, the main goal is to produce PLA based filaments that in comparison with fossil-based filaments have properties that are similar, or even better. Since the 3D printing market is mainly dominated by filaments of PLA and ABS[3], the properties of these two materials are compared in order to decide what properties to focus on when improving PLA.

The brittleness of PLA, which in Table 1.1 is represented by the low impact strength and low elongation at break, is the most problematic property. The ultimate tensile strength, on the other hand, is slightly higher for PLA than for ABS, which makes it possible to impel a trade-off between the ultimate tensile strength and the elongation in order to improve the overall function of PLA for application in 3D printing.

Table 1.1: Comparison of some thermal and mechanical properties of ABS and PLA[9, 10, 11, 12].

Properties	ABS	PLA
Ultimate tensile strength*	36.4 MPa	46.8 MPa
Elongation at break	3.5-50%	6%
Impact strength (Charpy impact, notched)*	25.6 kJ/m^2	7.80 kJ/m^2
Glass transition temperature, T_g*	108°C	59°C
Melting temperature, T_m	N/A (amorphous)	160°C
Melt flow index, MFI*	4.9 g/10 min	14.3 g/10 min

* Average value

PLA has a lower glass transition temperature compared to ABS. This is not an issue if the printed product is stored at room temperature since the T_g is sufficiently higher than room temperature. However, it might become a problem if the additives induce a reduction of T_g, especially if the final product must withstand higher temperatures. The glass transition temperature is therefore a property of the compounds that needs to be investigated.

An important parameter in 3D printing is the viscosity of the melted filament. The viscosity of the material affects parameters such as the adhesion between each layer and the shape of the printed product[13]. A high viscosity can cause clogging in the nozzle of the 3D printer[13] while a low viscosity instead can lead to incapacity to form the needed extrusion pressure[14]. The viscosity of a polymer melt is not a fixed value, it depends on the temperature and the applied shear rate, among others[15]. One way of predicting the flowability is to measure the melt flow index

(MFI) since it indicates how fast a melted polymeric material flows[13]. One study concluded, even though the melt flow index solely did not affect the printability, that a MFI>10g/(10 min) for PLA compounds is needed in order to successfully print the material[13]. Pure PLA already possesses this type of flow index range, and since the MFI is inversely proportional to the viscosity of the melt, it can be concluded that the viscosity of PLA should most desirably not be changed by the addition of additives.

To conclude, the requirements of the additives can be summarized as the following:

- bio-based
- economically sustainable
- exist as a commercial product
- no prior chemical modifications needed

and the desired properties of the produced compounds can be summarized as the following:

- increased elongation at break
- no or small reduction of tensile strength
- increased impact strength
- no or small reduction of T_g
- viscosity suitable for 3D printing

2
Background

In this chapter some theory of the thermal and mechanical properties of polymers will be introduced. The state of the art regarding modifications of PLA will also be presented as well as an overview of 3D printing and the methods used in the project.

2.1 Polymers

A polymer chain is a macromolecule which consists of several repeating units, monomers, that could be the same or different and acts as building blocks to construct the molecule[15]. The polymer chains are said to be crystalline if they are packed in an ordered structure exhibiting a long-range order while they are amorphous if the chains are randomly coiled, not exhibiting a long-range order[15]. A polymer matrix can be completely amorphous but not completely crystalline, instead different degrees of crystallinity can occur in a semi-crystalline polymer, which consists of both amorphous and crystalline regions[15].

2.1.1 Thermal properties

At sufficiently low temperatures all polymers are solids, but upon heating the material eventually gains enough thermal energy to enhance the mobility of the chains and behave like a viscous liquid[15]. If the material is completely amorphous, the temperature at which this transition occurs is called the glass transition temperature, T_g[15]. If the material is semi-crystalline, only the amorphous regions soften at T_g and the crystalline regions become liquid-like when reaching the melting point, T_m[15].

The glass transition is a kinetic process, hence the T_g is not a fixed temperature[15]. The T_g depends, among other parameters, on the heating or cooling rate at which it is observed and therefore different measurement methods can lead to different values[15]. The T_g of a polymer blend can be predicted using the Fox equation, Equation 2.1[5].

$$\frac{1}{T_g} = \frac{W_1}{T_{g1}} + \frac{W_2}{T_{g2}} \tag{2.1}$$

The T_g of the blend depends on the T_g of each individual polymer (T_{g1} and T_{g2}) and the weight fraction of each polymer in the the blend (W_1 and W_2)[5]. A blend that shows a single T_g in-between the two individual T_g values, in line with the predicted

value, indicates a miscible blend whereas a T_g that is not in line with the predicted value or a blend with two T_g values indicates an immiscible blend[5].

The degree of crystallinity in a polymer can vary depending on how the crystallization process is performed[15]. The crystallization is controlled by the temperature at which the sample is processed as well as the cooling rate after processing[15]. The rate of crystallization for a semi-crystalline polymer reaches a maximum in-between the T_g and the T_m[15]. This is because at temperatures around T_m the segmental motions are too great whereas close to T_g the motion of the chains is too slow to allow the chains to order into crystal structures[15]. The crystallization rate also depends on the polymer itself. Some polymers crystallize very fast and can therefore reach a high degree of crystallinity despite a high cooling rate, while some polymers crystallize more slowly and require a slower cooling rate in order to reach the same degree of crystallinity[15]. This means that a polymer melt that is cooled fast enough can become completely amorphous, even though it would be possible to crystallize the polymer at a lower cooling rate[15]. Factors that can influence the crystallinity are for example, the symmetry of the chains, the tacticity and the branching of the chains[15].

The heat resistance of a polymer is related to the crystallinity of the material[16]. A high degree of crystallinity means that upon heating to above T_g the stiffness of the sample is preserved, and therefore the material can withstand higher temperatures without being deformed[16].

2.1.2 Mechanical properties

Several important mechanical properties of a polymer can be measured from a stress-strain diagram resulting from a tensile test, see Figure 2.1. The stress corresponds to the tensile force applied onto the material during a tensile test and the strain is the resulting deformation, or extension, of the material[15].

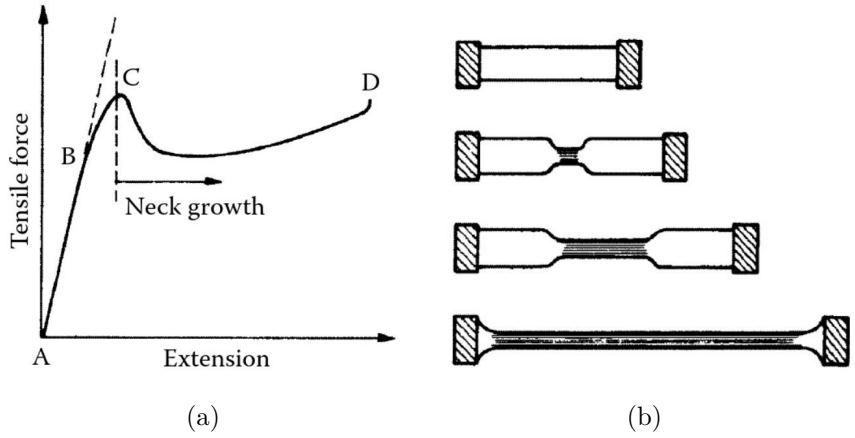

Figure 2.1: a) A stress-strain diagram resulting from a tensile test and b) the necking of the test specimen during plastic deformation[15].

The first linear part of the curve (point A-B) represents the elastic deformation, which is the deformation that the material can withstand and still regain its original shape when the tensile force is released[15]. The slope of this linear part of the curve is the modulus of elasticity or Young's modulus, denoted E, which is a measure of the stiffness of the material[15]. Point C is the yield point, defined as the maximum point of the curve[17]. The second part of the curve (point C-D) is where the plastic, irreversible, deformation takes place[15]. The area under the curve in the stress-strain diagram corresponds to the toughness of the material[15].

A brittle polymer will fracture at a low strain when the elastic deformation is exceeded, showing no or only a small plastic deformation[15]. A more ductile polymer will exhibit a yield point and then continue to deform as the necking occurs[15]. This means that the test specimen starts to taper from its center, as illustrated in Figure 2.1[15]. As the tensile force continues the tapered part, the neck, grows as a result of the increased chains alignment in the neck[15]. This alignment will result in a harder material, which is why this process is called strain hardening[15]. Due to the alignment of the chains the stress in the material will slightly decrease, but eventually it will build up again as the chains reach their maximum contour length[15]. At this point test specimen fractures[15].

The mechanical properties that a plastic material exhibit depends on for example the molecular structure of the chains, entanglements and cross-links but it is also temperature dependent[15]. When the temperature increases the tensile strength and the rigidity decreases, which means that a brittle polymer will transform and become softer upon increased temperature[15].

2.1.3 Polylactic acid

Polylactic acid is a bio-based polymer, and more specifically, a linear thermoplastic polyester[4]. The chemical structure of PLA is presented in Figure 2.2. PLA is both biodegradable and biocompatible and considering its high strength and modulus of elasticity it can be used in applications such as disposable materials, medical devices and food packaging[4].

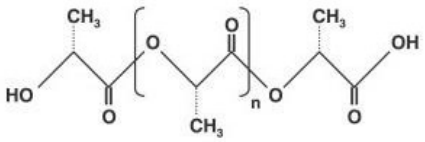

Figure 2.2: The chemical structure of polylactic acid[18].

PLA is transparent in its neat form and can be both amorphous and semi-crystalline due to the two enantiomers of the lactic acid monomer, L-lactic acid and D-lactic acid[18], which are presented in Figure 2.3. PLA is synthesized via two different routes; condensation of lactic acid or ring-opening polymerization of lactide, which also originates from lactic acid[19]. The lactide molecule comes in three structures, presented in Figure 2.3. The DD-lactide is produced from only D-lactic acid,

LL-lactide is produced from L-lactic acid and LD-lactide, also called meso-lactide, is produced from a combination of D- and L-lactic acid[19]. The PLA produced from pure D-lactic acid and pure L-lactic acid is referred to as PDLA and PLLA respectively[19]. Commercial PLA is usually based on a mixture of the both enantiomers, L-lactic acid being the dominant one[19]. The completely amorphous PLA consist of at least 20% D-lactic acid monomer, while the semi-crystalline PLA has a lower content of D-lactic acid[19].

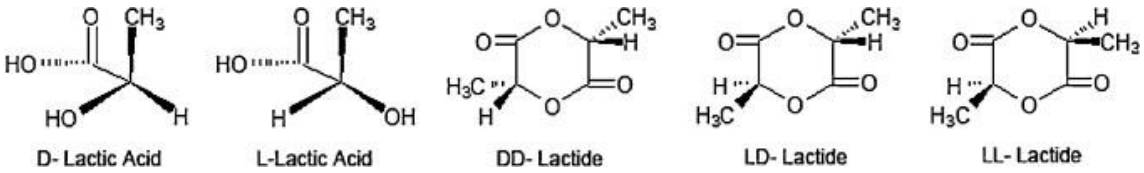

Figure 2.3: The structures of the two enantiomers of lactic acid and the three structures of lactide based on lactic acid[19].

There are several types of PLA crystals; α, α', β and γ, all exhibiting a helical chain conformation[19]. The α structure is the most commonly occurring while the α' structure, which is created by annealing at temperatures below 100°C, is similar to the α structure but is less densely packed and has a less ordered chain structure[19]. These two structures can coexist and can be seen in a DSC curve as two melting peaks, the one having a lower temperature resulting from the melting of α' crystals and their recrystallization to α crystals, and the other as the melting of the α crystals[20]. The β structure is found by stretching the α structure at high temperatures and its melting point is slightly lower than the α crystals[19]. The γ crystal is a more ordered type of crystal where two chains are ordered antiparallel in the conformation[19]. These types of crystal structures results from the crystallization of PLLA or PDLA, but when both types exist in a blend, the chains can co-crystallize resulting in a stereocomplex[19]. This stereocomplex has a higher melting point than the homo-crystals which provides the material with a higher heat resistance[19].

The crystal content of the polymer affects its properties to a large extent. A higher crystalline content will improve the thermal resistance but at the same time it has been shown that the enzymatic degradation rate is reduced, which affect the biodegradability of the polymer[19].

PLA is also hygroscopic meaning that it absorbs moisture from the atmosphere[21]. This moisture results in hydrolysis of the polymer, and reduction of the molecular weight which affects for example the melt viscosity and mechanical properties[21].

2.2 Modification of mechanical properties of PLA

Many attempts have been made to modify the properties of PLA, especially with focus on the brittleness, by combining PLA with different types of additives. The attempts have sometimes been with the focus on 3D printing filaments while other

have been of a more general nature. This section presents a study of the current research regarding modifications of PLA with respect to its mechanical properties followed by modifications to increase the heat resistance.

2.2.1 Plasticizers

Plasticizers are small molecules introduced to the polymer matrix to enhance the ductility of the polymer[22]. The most widely accepted theories of the mechanisms behind plasticizing are the lubricity theory and the gel theory[23]. According to the lubricity theory, the plasticizer reduces the friction between the polymer chains and therefore enhances the chain mobility while the gel theory interprets the enhanced ductility as the disruption of polymer-polymer interactions and the introduction of new plasticizer-polymer interactions which results in increased flexibility of the polymer chains[23]. Hence, the addition of plasticizers increases the chain mobility and flexibility, but as a consequence less energy is needed to break the remaining interaction between the chains in the amorphous configuration[22]. Thus, the glass transition temperature and the rubbery plateau modulus are lowered which leads to the softer feeling of plasticized polymers[22].

The addition of plasticizers is a cost-effective way to improve the ductility of a polymer but the low molecular weight and high mobility of the plasticizers can induce migration of the plasticizers from the bulk to the surface of the polymer[24]. This can decrease the durability of the plasticized polymer since it will regain its brittleness as the plasticizer migrates to the surface[24].

2.2.1.1 Vegetable oils

Some studies have showed success in increasing the elongation at break from 5% for pure PLA up to as much as 220% by compounding PLA with modified vegetable oils, but a decrease in tensile strength from 60 to approximately 30 MPa also appeared[8, 23]. Vegetable oil plasticizers are of interest since they are cheap, abundant, bio-based and biodegradable[23]. The use of unmodified vegetable oils in the PLA compounds was reported to cause compatibility issues in the compound, but chemical modifications such as maleinizing or epoxidizing gave the oils a more suitable solubility parameter as the polarity was increased[8].

The modified vegetable oils did not only change the mechanical properties, they also improved the thermal stability by increasing the degradation onset temperature from 274°C for pure PLA to 330°C[23]. As a result of the enhanced chain mobility, the glass transition temperature decreased, but only a reduction of maximum of 6.4°C was reported, from 65.4°C of neat PLA to 59.0°C, which occurred when 20 phr (part by weight of oil per 100 parts by weight of PLA) of malenized linseed oil was added[8].

In previous studies within the project led by Add North, 5 wt% unmodified linseed oil together with 5 wt% thermoplastic polyurethane were compounded with PLA[25]. This resulted in a compound with increased Charpy impact strength (notched) from 2.4 kJ/m^2 to 2.9 kJ/m^2 and increased elongation at break from 5% to 11% compared

to pure PLA[25]. By adding slightly more PLA to the composition, the compound also showed promising printing properties[25]. Unmodified linseed oil alone was also compounded with PLA but it was not possible to investigate the mechanical properties of the compound because of its oiliness, probably due to phase separation of the compound[25].

2.2.1.2 Citrate esters

Different types of citrate esters have also been investigated as plasticizers in pure PLA and in PLA composites[26, 27]. The chemical structures of two commonly used citrate esters, acetyl tributyl citrate and triethyl citrate are illustrated in Figure 2.4. Citrate esters are nontoxic, biodegradable and sometimes bio-based, and they are also compatible with PLA due to polar interactions between the ester groups in the two components[28].

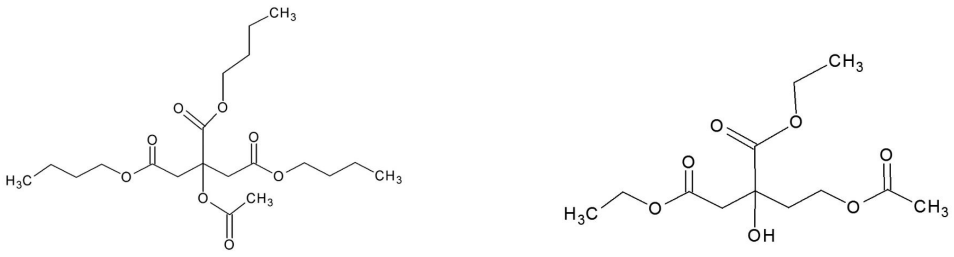

(a) ATBC (b) TEC

Figure 2.4: The chemical structures of a) Acetyl tributyl citrate, ATBC, and b) Triethyl citrate, TEC[28].

Both amorphous and semi-crystalline PLA were investigated together with the citrate esters and the studies showed similar results. The citrate esters efficiently increase the elongation at break meanwhile decreasing the tensile strength, regardless of what type or the amount (10-30 wt%) of the citrate ester added[26, 27]. By compounding PLA with 10 wt% ATBC, an elongation at break of 46% was reached and the tensile strength was decreased from 41 to 18 MPa[26]. As a consequence of the addition of plasticizers, the T_g is lowered, and in the case of citrate esters, addition of only 10 wt% can lower the T_g to around room temperature[26].

Few investigation on the impact strength of these compounds have been conducted, but one study has taken the melt flow index into account. This study has showed that an addition of 10 wt% ATBC or TEC increases the melt flow index of pure PLA from 5 g/10 min to approximately 10 g/10 min[28].

2.2.2 Elastomers

The most distinguishable feature of elastomers is their unique ability to deform elastically, exhibiting an elongation up to several hundred percent[15]. Most polymers exhibit a limited elastic deformation since the elasticity and the ability to regain the

original shape relates to the movement of atoms from their equilibrium condition[15]. Elastomers, on the other hand, consists of a cross-linked matrix or polymers with a molar mass large enough to form a network which provide the elastomers with the ability to recover from a major elongation[15]. Elastomers have in principle no crystallinity and they are used well above their T_g[15].

2.2.2.1 Core-shell rubber and natural rubber

Great success in modifying PLA composites with respect to their brittleness has been achieved using core-shell rubber particles[4, 29, 30]. The addition of 10 wt% core-shell rubber reduces the tensile strength of pure PLA from 68 to 54 MPa, increases the elongation at break from 4.7% to 7.0% and increases the impact strength from 15 kJ/m^2 to 111 kJ/m^2[4]. Core-shell rubber particles consists of a crosslinked elastomeric core and a thermoplastic shell[30]. The core of the particles is said to be responsible for giving the composite its increased ductile behavior whereas the shell enables good dispersion of the particles in the polymer matrix[4, 30]. The origin of these rubber particles were in some studies not stated, while some of them are known to be fossil-based[4, 29, 30].

To maintain the bio-based characteristics of the PLA compounds, natural rubber has been investigated as an additive[31]. The difference in polarity of natural rubber and PLA have led to the addition of compatibilizers, modifications of the rubber or copolymerization of PLA and the rubber to enhance the miscibility[31]. When pure natural rubber was compounded with PLA, the SEM images of the compound revealed large cavities generated by the rubber[31]. These cavities were believed to work as energy absorbers as the Izod impact strength of this compound increased to 51.3 J/m compared to 28.9 J/m for neat PLA[31]. This compounding also resulted in a lowering of the tensile strength, from 56.1 MPa to 26.4 MPa, as well as of the elongation at break, from 11.2% to 6.8%, which were believed to be caused by the phase separation in the compound[31]. However, the use of copolymerized and modified rubber showed the same trends, so the presumed increased compatibility was not enough to increase the the elongation at break[31].

2.2.2.2 Thermoplastic polyurethane

Thermoplastic polyurethane (TPU), has also been investigated as an additive to decrease the brittleness of PLA. TPU is an elastomer that consists of both soft and hard segments[32]. The soft segments, which are based on either polyester or polyether, are mostly present in amorphous conformations with a low T_g which give the material its flexibility while the hard segments of diisocyanate and diols provide the materials with its high strength[32, 33]. In several studies, the addition of TPU increased the elongation at break and the impact strength while the tensile strength only slightly decreased with the addition of TPU[32, 33]. For example, when 20 wt% TPU was added to PLA, the elongation at break increased from 1.0% for pure PLA to 2.5%, the impact strength increased from 5 kJ/m^2 to 16 kJ/m^2 and the tensile strength was decreased from 37.9 MPa to 33.8 MPa[33]. The thermal characterization showed two T_g values for the compounds, one for TPU and one for

PLA[32, 33]. The T_g of PLA was slightly decreased by the addition of TPU, with a maximum decrease of 10°C, from 57.5°C to 47.7°C, which occurred when as much as 50 wt% TPU was added[33]. The compounds with the addition of up to 10 wt% TPU showed no decrease in T_g [32, 33].

TPU as an additive was investigated in the project led by Add North in mixture with linseed oil. TPU alone was also investigated in that project which by the addition of 10 wt% showed promising properties, for example an increased impact strength and increased elongation at break[25].

2.3 Modification of heat resistance

In addition to an increased ductility, PLA would also profit from an increased heat resistance[34]. The heat resistance of a material can be determined by the heat deflection temperature, HDT, which depends on the crystallinity of the material[16].

Different additives can be used to facilitate the crystallization. When plasticizers are added to the polymer, the chain mobility is increased which means that less energy is needed to order the chains into crystals[16]. Plasticizers can therefore enhance the crystallization rate of the polymer[16]. Nucleating agents, such as talc, can also be added to induce crystallization[16].

Different types of fibers such as bamboo and cellulose fibers have also been added to improve the heat resistance[16]. When adding fibers, the heat deflection temperature is increased partly due to a higher HDT of the fiber compared to the polymer matrix and partly because the fibers act as nucleating agents[16]. These natural fibers also increase the tensile strength of the compound by acting as reinforcement in the matrix[35]. They can also increase the impact strength but the elongation at break is usually lowered as a result of the increased tensile strength[35].

The addition of additives to facilitate crystallization is not enough to increase the heat resistance unless the material is actually crystallized. This is controlled by the temperature at which the sample is processed as well as cooling rate used after the processing[15]. Annealing after the processing, i.e. heating the material for a certain time to the temperature span where crystallization occurs, can also be used to increase the crystallinity and hence the heat resistance[15].

2.4 3D printing

3D printing is an umbrella term for several types of printing techniques; fused deposition modeling (FDM), stereolithography (SLA) and selective laser sintering (SLS) to name a few[2]. FDM can be used in many industries but it has grown to become a popular technique for prototype printing at home[36] and it is the most common technique when printing polymeric materials[2].

In FDM, the material used is a filament which is an advantage over the other 3D printing methods since it offers flexibility for printing[2]. When printing, the filament is fed by rollers into the liquefier chamber of the nozzle where it melts, and the melt is then extruded and deposited by the nozzle onto a substrate, a bed, to create the printed object[2]. This process is illustrated in Figure 2.5.

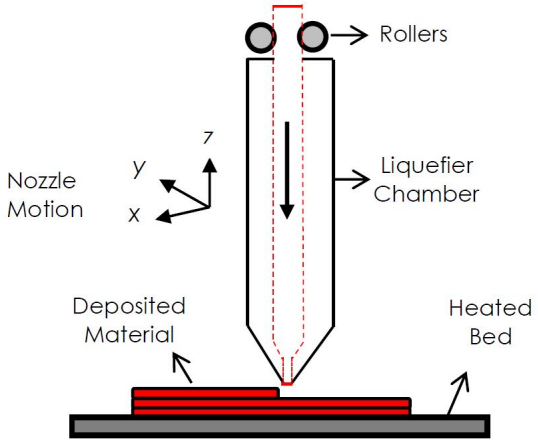

Figure 2.5: A schematic illustration of how the filament is extruded through the nozzle to generate the printed layers[37].

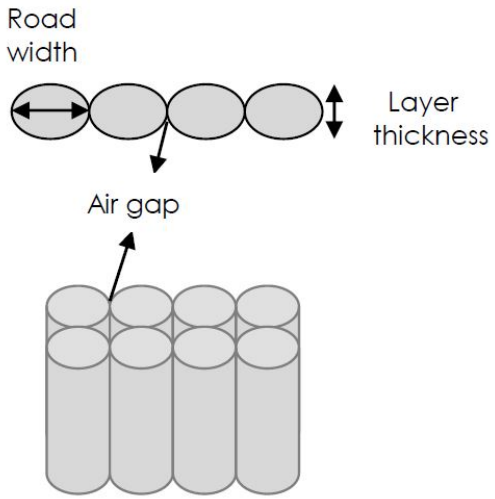

Figure 2.6: An overview of the printed layers and possible air gaps in the print[37].

The temperature is an important parameter when printing[36]. The filament needs to be melted in order to be shaped and to adhere to the adjacent layers in the printed product[36]. Too much heat can however lead to deformations in the product, since the viscosity can be reduced and the cooling time increased due to the elevated temperature, which means that the material will be too soft to withstand the weight of the superjacent layers[36]. A higher viscosity of the material leads to better control of the layer thickness, but it can also lead to air gaps between the layers as illustrated in Figure 2.6[36]. It is not only the temperature that determines the behavior of the deposited material, the viscosity of the material itself also plays an important role[36].

Several additional parameters can also be adjusted to optimize the print, for example the printing rate and the thickness of the layers, called the bed level, which is the distance between the nozzle and the bed[37]. To get a good print, it is important to have a consistent road width, i.e. the width of the printed layer. This is achieved by minimizing the pressure drop in the nozzle, which in turn is determined by the nozzle diameter[37]. A larger diameter results in a lower pressure drop and therefore a more consistent print[37]. A larger nozzle diameter can also reduce the printing time but a smaller nozzle diameter can print smaller details and more precisely[37]. Different nozzle diameters can be found on the market but a diameter of 4 mm is common[37].

2.5 Experimental methods

The following section describes the theory behind the methods used to prepare and characterize the compounds.

2.5.1 Extrusion

Extrusion is a technique for processing and blending polymeric materials, in which the material is continuously processed by the rotation of one or two screws in a heated barrel[38]. The material is added as solid pellets to the extruder via the feed hopper, and as the material melts in the barrel the screw mixes the melt into a homogeneous blend and transports it through the barrel[39]. The final blend, called extrudate, can have different shapes depending on the die used in the end of the extruder[39]. In the single screw extruder only one screw is used while the twin screw extruder uses two screws. The twin screw extruder enables improved mixing and the screws can be rotated in the same direction or counter rotated[38].

2.5.2 Injection molding

Injection molding is a process used to produce samples of a certain shape by pressing the material into a pre-decided mold[39]. Similar to extrusion, the material is fed as pellets into a heated barrel containing a rotating screw[39]. The material melts and under high pressure the screw forces the melt into the mold which is attached to the end of the barrel. After the cooling procedure the mold is opened to obtain the final sample[39].

2.5.3 Differential scanning calorimetry

When a sample undergoes a physical or chemical change, a change in the enthalpy also occurs[15]. This change in enthalpy can be observed using differential scanning calorimetry, DSC[15]. The DSC instrument consists of two individual heating chambers where the sample is placed in one of them and the other is used as a reference[15]. The chambers are simultaneously heated at the same rate and the same temperature is kept in the chambers which is controlled by monitors in each chamber [15].

When the sample exhibits a change in enthalpy, the temperature in that chamber is temporarily reduced or increased depending on the nature of this enthalpy change[15]. The system therefore increases the energy input to the chamber if an endothermic reaction occurs, and reduces the energy input if an exothermic reaction occurs, to compensate for the temperature change[15]. The energy input is monitored which makes it possible to observe the energy augmentations and reductions as a function of temperature, i.e. different exothermic and endothermic events in the sample such as crystallization and melting[15].

2.5.4 Capillary viscometry

To measure the viscosity of a polymer melt a capillary viscometer can be used[40]. The instrument consists of a heated cylinder where the material is loaded at the top[41]. At the bottom of the cylinder a capillary die, with a certain length (L_c) and diameter of the capillary ($2R_c$), is attached[41]. The area of the die is equal to the cross section of the cylinder (A)[41]. When conducting the measurement the material is melted to a pre-determined temperature and a piston presses the material through the cylinder and through the capillary meanwhile a pressure transducer measures the force (F) needed to press the material through the capillary[40]. The speed of the piston can be increased in different steps, but the speed in each step is kept at a constant rate (v)[40]. An illustration of a capillary viscometer is presented in Figure 2.7.

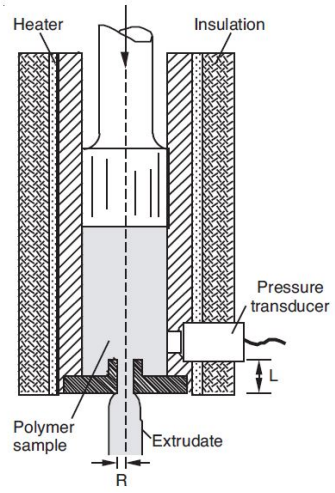

Figure 2.7: An illustration of a capillary viscometer showing the heated cylinder with the capillary die at the bottom, the pressure transducer and the piston pressing the melt trough the cylinder[40].

From the known and measured parameters, the shear stress (τ) and shear rate ($\dot{\gamma}$) are calculated using Equation 2.2 and Equation 2.3, where Δp=F/A is the pressure drop and Q=v×A is the volume flow[41]. The viscosity (μ) can thereafter be calculated from the shear stress and shear rate using Equation 2.4[41].

$$\tau = \frac{\Delta p R_c}{2L_c}[Pa] \tag{2.2}$$

$$\dot{\gamma} = \frac{4Q}{\pi R_c^3}\left[\frac{1}{s}\right] \tag{2.3}$$

$$\mu = \frac{\tau_w}{\dot{\gamma}_w}[Pas] \tag{2.4}$$

When the material is pressed into the capillary, a deformation of the material occurs which is related to pressure losses, but since the pressure transducer cannot be placed inside the capillary, these losses are not monitored[40]. The obtained values of the

shear stress, shear strain and viscosity are therefore the apparent values, but it is possible to calculate the so called corrected values from the apparent values[40]. The correction for the pressure losses is calculated using the Ryder-Bagley correction, but it is also possible to consider non-Newtonian behaviors using the Weissenberg-Rabinowitsch correction[40].

2.5.5 Impact test

An impact test is used to measure the impact strength of a material, i.e. its ability to absorb mechanical impact energy[42]. The instrument consist of a pendulum that is released from its starting position, swings in a half-circle and impacts the test specimen which is mounted at the base of the instrument, as illustrated in Figure 2.8. The difference between the kinetic energy which the pendulum possesses at its starting position respective to its final position is equal to the energy that the test specimen has absorbed[42]. This energy is measured by the instrument[42].

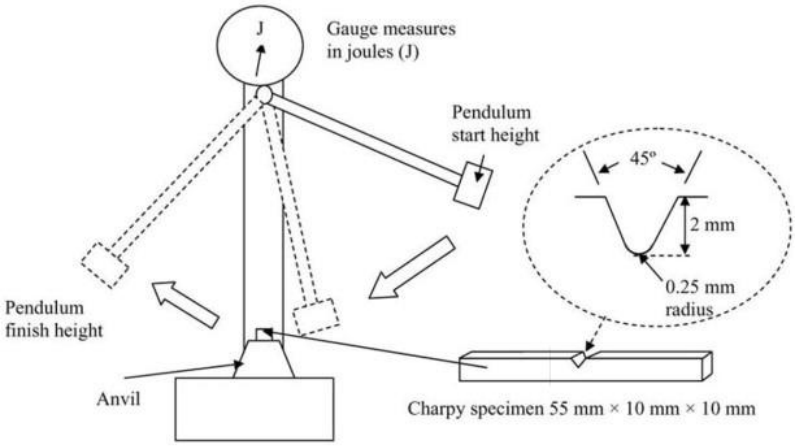

Figure 2.8: An illustration of a Charpy impact test[42].

An impact test can be executed in different set-ups, such as a Charpy impact test and an Izod impact test, Charpy being the more common one[42]. The difference between the tests is the size of the test specimen and the direction of which the specimen is placed in the instrument[43]. In a Charpy test, the specimen is placed horizontally fixed by two clamps, the pendulum hits the specimen in its center while the specimen in an Izod test is place vertically, fixed at the lower part by a single clamp, and the pendulum hits the upper half of the specimen[43].

In Charpy impact test, the test specimen can either be placed edgewise of flatwise, as in Figure 2.9. The flatwise is most commonly un-notched whereas the edgewise can be either notched or un-notched. In the Charpy test the notch is turned away from the pendulum while in Izod test the notch is facing the pendulum[43].

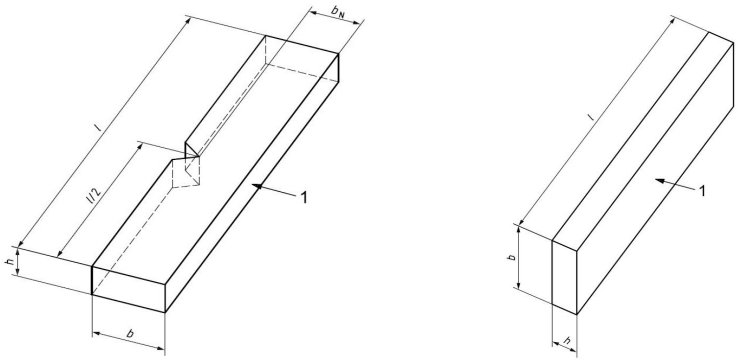

(a) Charpy Edgewise Impact (b) Charpy Flatwise Impact

Figure 2.9: The two sample configurations of Chapry impact test: a) Edgewise, and b) Flatwise. The edgewise sample is notched whereas the flatwise is un-notched. The arrow marked 1 represents the direction from which the pendulum hits the specimen[44].

2.5.6 Tensile test

A tensile test is conducted by applying a tensile force at constant strain rate onto the test specimen, i.e. pulling the test specimen in opposite directions[15]. The mechanical properties of the material can be determined from monitoring the resistant force and the deformation of the material during the test[15]. The recorded data can be processed according to Equation 2.5 and 2.6[17]. In Equation 2.5, σ is the stress (Pa), F is the recorded force (N) and A is the cross section of the sample (m^2)[17]. In Equation 2.6, ϵ is the strain (%), ΔL is the change in length (mm) and L_0 is the original length (mm) of the specimen[17].

$$\sigma = \frac{F}{A}[Pa] \tag{2.5}$$

$$\epsilon = \frac{\Delta L}{L_0}[\%] \tag{2.6}$$

The elastic modulus (E), which is the slope of the initial linear part of the curve, is calculated according to Equation 2.7[17].

$$E = \frac{\Delta\sigma}{\Delta\epsilon}[Pa] \tag{2.7}$$

3
Methodology

In this section a short description of the materials used in the compounds is presented followed by the experimental details of the preparation and characterization of the compounds.

3.1 Materials

The PLA used in all the compounds is Inego™ Biopolymer 4043D (D enantiomer content approximately 5%[45]) obtained from NatureWorks. The additives used are an acetyl tributyl citrate, ATBC, called CITROFOL® BII obtained from Jungbunzlauer and a thermoplastic polyurethane, TPU, called Pearlthane® ECO 12T95, obtained from Lubrizol. The motivation for why these additives are used is presented in Section 4.1

3.2 Preparation of compounds

The raw materials used for the compounds are shown in Figure 3.1. The materials were dried over-night in a Moretto SX Sincro Dryer at 40°C as a pre-treatment before extrusion to remove any possibly absorbed moisture. The PLA and TPU were dried separately, their amounts were measured then mixed together by hand prior to extrusion. For the compound containing ATBC, the additive was blended with the PLA prior to drying.

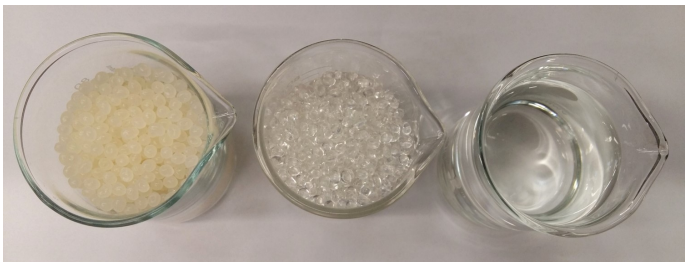

Figure 3.1: The raw materials used to prepare the compounds. Left to right: PLA pellets, TPU pellets and the liquid ATBC.

The composition of each compounds is presented in Table 3.1. The total weight of each compound batch was 3.5 kg and the additives were added to the PLA on the basis of weight percentage.

Table 3.1: The composition of each compound.

Compound	PLA [wt%]	ATBC [wt%]	TPU [wt%]
PLA	100	0	0
PLA+2%ATBC	98	2	0
PLA+2%TPU	98	0	2
PLA+5%TPU	95	0	5
PLA+12%TPU	88	0	12

A single screw extruder, Brabender compact extruder, with a dispersion screw and a circular die (1.5 mm in diameter) was used for the extrusion. The barrel consists of three heating zones and the die can be seen as a forth zone. The temperature profile used for all compounds were 180-200-200-210°C (zone 1-4). The screw speed was set to 25-30 rpm. The temperatures and the screw speed was monitored using the WINExt software.

After extrusion the extrudates were pelletized using a Dreher pelletizer. The compounds containing additives were extruded twice in order to get a good dispersion of the additives in the polymer matrix.

3.3 Preparation of specimens for mechanical tests

The specimens needed for the mechanical tests were produced by injection molding, using an Arburg Allrounder 221M 250-55. The pelletized extrudates were used for the injection molding, except for pure PLA for which the unextruded pellets were used. Prior to injection molding, all the compounds were dried over-night in a Moretto SX Sincro Dryer at 40°C, except PLA+2%ATBC which was dried at 60°C in a Heraeus D-6450 Hanau vacuum oven, to remove any absorbed moisture. Some compounds contained larger pellets. These pellets were removed prior to injection molding.

The temperature profile of the barrel was 120-140-160-180-200°C. The injection pressure was 900 bar, the holding pressure was 550 bar for 3 s followed by 400 bar for 17 s and the cooling time was 30 s. The shot volume was set to 20 cm^3 and each shot was manually loaded by rotating and moving the screw inside the barrel prior to injection. The loading and injection cycle was repeated until the number of needed test specimens were produced.

3.4 Differential scanning calorimetry

The samples were prepared by cutting a small piece (5.0 - 5.5 mg) of the pelletized extrudates, and each sample was placed in an aluminum crucibles of 25 µl. All

the compounds was investigated as well as pure TPU as a reference. The samples were exposed to a temperature cycle which started with an isothermal treatment for 2 min at 20°C, then the temperature increased from 20°C to 280°C at a rate of 10°C/min and lastly the temperature decreased down to 20°C using the same rate. This temperature cycle was run twice with an isothermal treatment for 1 min at 20°C in-between. The measurements were performed under a nitrogen atmosphere. The instrument used was a Mettler DSC 2 together with the software STARe System.

The same procedure was also used for a measurement at a lower heating rate, 5°C/min, but the instrument used for this measurement was a Perkin Elmer DSC 7 and the software used to set the parameters was Pyris series DSC 7.

3.5 Capillary viscometry

The viscosity of the compounds was measured using a Göttfert Rheograph 2002. The parameters were set up and monitored using the LabRheo software. The temperature was set to 200°C and the piston speed was set according to Table 3.2, which also shows the corresponding shear rate. The piston speed was automatically increased to the next level when a steady pressure was reached, or when 600 s had passed. At each level a constant speed was kept. A capillary die with a diameter of 0.5 mm and a length of 10 mm was used.

Table 3.2: The piston speed and the corresponding shear rate used when measuring the melt viscosity of the compounds.

Piston speed [mm/s]	shear rate [s^{-1}]
0.01	92.2
0.02	184.3
0.04	368.6
0.06	553.0
0.08	737.3
0.10	921.6
0.12	1105.9
0.14	1290.2
0.16	1474.6

Prior to measuring the instrument was heated, the pressure transducer was calibrated and the material, which was dried overnight at 40°C in a Heraeus D-6450 Hanau vacuum oven, was fed as pellets into the cylinder. The piston was manually pulled down through cylinder to compress the material. This was repeated several times and more material was fed into the cylinder between each compression to make

sure that the cylinder was filled with densely packed material. Two measurements for each material were then executed.

3.6 Impact test

Prior to the test, the specimens were prepared by marking the middle of each specimen to ensure that the pendulum of the impact tester would hit every specimen at the same place. The specimens were then placed in a conditioning box at 23°C with 55% relative humidity for 3 days before testing. The Impact test was performed as a flatwise, un-notched charpy impact test according to ISO 179 with the exception that the specimens where shaped as dogbones and not bars. Five specimens of each compound were tested and a mean value of the impact strength was calculated.

The impact tester measured the energy absorbed using the unit kpcm, which can be converted to joules according to Equation 3.1. The impact strength was calculated using Equation 3.2.

$$1kpcm = 0,0981Nm = 0,0981J \tag{3.1}$$

$$\text{Impact strength}[J/m^2] = \frac{\text{energy absorbed}[kpcm] \times 0,0981[J]}{\text{cross sectional area}[m^2]} \tag{3.2}$$

To determine the cross sectional area of each test specimen, the width of the specimen and the thickness of the edge was measured at the mark using a Mitutoyo micrometer. The resulting thickness of the specimen was found by measuring how the thickness in the center of the specimen deviated from the thickness at the edge using a C.E. Johansson 8336-20 dial gauge and then the resulting thickness was calculated by subtracting the deviation at the center of the specimen from the thickness measured at the edge.

3.7 Tensile test

Before measuring, the specimens were placed in a conditioning box at 23°C with 55% relative humidity for 3 days. The tensile test was performed using an Instron 4505-5500R tensile tester. Five specimens of each compound were tested. A grip to grip separation of approximately 110 mm, a grip pressure of approximately 50 bar, a pre-load of 1 N and a strain rate of 5 mm/min were used. The software Instron Bluehill was used to record the force and extension data.

The cross sectional area of each specimen was found using the same procedure as described in Section 3.6. The specimens were measured at five points and a mean for each specimen was calculated.

4
Results and discussion

This chapter begins with an evaluation of the state of the art additives for PLA compounds together with a motivation for why the additives used in this project were chosen. This is followed by the results from the preparation and characterization of the compounds, presented together with an interpretation and discussion of the result.

4.1 Evaluation of state of the art additives for PLA compounds

Evaluating the current research regarding the modifications of the brittleness of PLA shows that several additives are promising for PLA compounds. The vegetable oils fulfill the requirement of being bio-based and have also showed to give the compounds the desired properties. The problem that arises when compounding PLA with vegetable oils is the compatibility. Modified oils seem to be more suitable for PLA compounds, but unmodified oil is less expensive, which also is an aspect to consider when choosing the additives. Even though the vegetable oil, for example linseed oil, is an interesting additive to investigate, it was not included in this project due to practical processing issues.

Citrate esters, another type of plasticizer, also fulfill all the requirements as an additive, and they have shown great potential at decreasing the brittleness of PLA. However, the simultaneous reduction of the T_g limits the amount of citrate ester that is possible to add to the compound. Since the addition of only 10% citrate ester resulted in a lowering of T_g down to room temperature it was decided that a very small amount, 2 wt%, of this additive would be investigated. The acetyl tributyl citrate was found to be completely bio-based which is why that type of citrate esters was used.

In addition to plasticizers, different types of rubber materials also exhibit promising properties as additives in PLA compounds. In particular, core-shell rubbers are of interest, but the lack of bio-based core shell rubbers hindered the investigation of this additive in the current project. Natural rubber could be a suitable substitute to core-shell rubbers, but due to the low miscibility with PLA this type of material was also excluded from this project.

Another type of elastomer, investigated in this project was TPU. The literature studies as well as the previous investigations within the project led by Add North have shown promising results regarding the ability of TPU to decrease the brittleness of PLA. This additive was therefore further investigated. Unlike the citrate esters, there was no maximum limit to take into consideration when adding TPU to PLA, which is why compounds with 2, 5 and 12 wt% TPU were investigated. The TPU used in this project is only 32% bio-based but since research regarding synthesis of a fully bio-based TPU is ongoing[46, 47] it is of interest to investigate this additive.

The state of the art methods used to increase the heat deflection temperature are either based on increasing the crystallinity or adding reinforcing materials to the matrix[16]. The addition of reinforcement is however usually in conflict with the desired improvement of the elongation at break.

When a filament is being 3D printed, its thermal history is deleted since the filaments is reheated during the printing process. The crystallinity of the printed product might therefore not be the same as in the filament. This means that the crystallinity of the final product is not only determined by the nucleating agent or additive in the polymer matrix but it is also determined by the printing conditions. Annealing the product to increase the crystallinity after printing can shrink the product. This is because the polymer chains in crystals are more densely packed compared to the amorphous state. This shrinkage must therefore be taken into consideration when designing the 3D model of the product. Due to complexity, the attempt to increase the heat resistance of the filaments using additives was postponed to a future study.

4.2 Preparation of compounds and test specimens

The pelletized extrudates of each compound is presented in Figure 4.1. A quite large size distribution of the pellets is observed, both within and between the compounds. The pure PLA exhibits the largest size distribution, probably resulting from being cooled down and stiff when pelletized. The other compounds were pelletized when still not completely cooled down which resulted in more flexible extrudates which were easier to be pelletized into more equal sized pellets. However, some larger pellets were obtained for each compounds, which for example can be seen in the beaker containing PLA+12%TPU in Figure 4.1.

The thickness of the extrudates also varies, PLA+12%TPU exhibiting the thickest pellets followed by PLA+5%TPU meanwhile PLA+2%TPU exhibits the thinnest pellets and pure PLA and PLA+2%ATBC exhibit similar thickness in-between the compounds containing TPU. The difference in thickness is most likely due to different die swell of the compounds and different feeding rate during the extrusion.

The longer pellets needed to be removed prior to injection molding to avoid blocking the inlet of the feed hopper and to ensure a steady flow of material. This was easily done for the compounds with fewer pellets of this larger size but for the pure PLA

the majority of the pellets were too large for the inlet. A mill was used in an attempt to cut the pellets into smaller pieces, but the mill needed substantial cleaning to remove old polymer residues before milling the pellets. This led to the decision not to use the pelletized extrudate when injection molding pure PLA, but use the raw material, i.e. the unextruded pellets, instead.

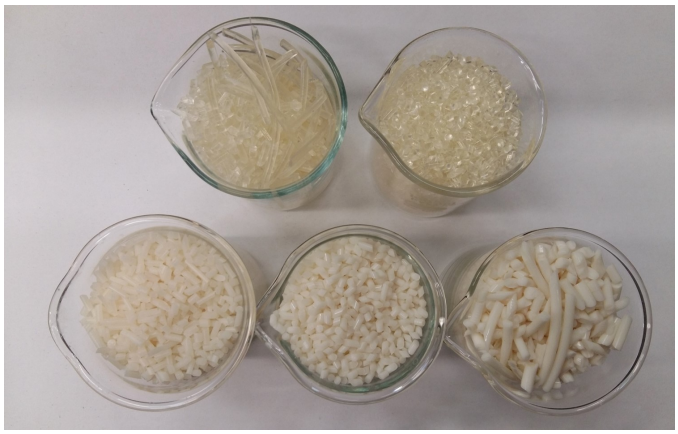

Figure 4.1: The pelletized extrudates. Upper row left to right: PLA and PLA+2%ATBC. Lower row left to right: PLA+2%TPU, PLA+5%TPU and PLA+12%TPU.

Figure 4.2: The injection molded samples. Left to right: PLA, PLA+2%ATBC, PLA+2%TPU, PLA+5%TPU, PLA+12%TPU.

One injection molded specimen of each compound is presented in Figure 4.2. The pure PLA and PLA+2%ATBC are transparent meanwhile the specimens containing TPU are opaque. With increasing content of TPU the appearance of these specimens changes from beige to white. Some shrinkage can be observed on the specimens, for example along the thinner part of the PLA+5%TPU. This shrinkage is present in almost every specimen, some specimen exhibiting a uniform shrinkage along the thinner part of the specimen while some specimens exhibiting a more uneven shrinkage of different depths along the specimen.

The polymer processing in this project was overall a troublesome procedure. The second extrusion of the compounds resulted in a high screw torque, especially for the TPU containing compounds. The extruder was disassembled for lubrication of the bearings and general cleaning which was somewhat efficient, but a slightly increased torque was still present. Since this behavior only occurred during the second extrusion of the compounds it is possible that the extruder struggled with the pelletized extrudates, since these pellets sometimes were larger and of a more uneven size than the raw materials.

Several issues also arose when injection molding. The most apparent issue was the shrinkage of the specimens. Several attempts to overcome this were made, mainly by adjusting the injection pressure, holding pressure, cooling time and shot volume. The shrinkage was only eliminated when a larger volume was injected, but then it was not possible to eject the specimens from the mold which resulted in bent specimens from pulling them out. A balance between minimum shrinkage and removable

specimens was eventually found, but some specimens still suffered from these defects.

The very first injection always needed to be loaded manually, but after that the instrument automatically loads a new shot of polymer melt for the following injection. This function enables the injection molding to be a continuous process, but when the compounds containing additives were injection molded the instrument was unable to automatically load a new shot of sufficient volume. The instrument indicated that a shot of sufficient volume was prepared, but the mold was not even filled to half. When the shot instead was loaded manually the mold was filled.

If the processing temperature was too close to the melting temperature it is possible that the compounds were not completely melted and therefore had a higher viscosity than expected, which could have affected the automatic loading. The DSC thermograms, presented in Section 4.3, did not indicate that this was the case. This matter was however investigated by increasing the temperature 20°C in each heating zone, but without success. The temperature of the melt was also measured using a heat camera to exclude that the thermo couples were miscalibrated, but that was neither the case. Despite several attempts, the problem with the loading was not solved which means that every specimen was produced by manually loading the shot volume.

The first attempt of injection molding PLA+2%ATBC did not only result in half-filled molds, it also resulted in samples containing bubbles or air pockets of various sizes. It is possible that absorbed moisture in the compound gave rise to these bubbles, hence the compound was re-dried at 60°C over-night. The second attempt showed no bubbles or air pockets, thus the second drying was successful.

Some alternatives to injection molding was considered, for example, cutting out test samples from extruded stripes. This idea was however rejected due to the belief that a sufficient thickness of the stripes would be difficult to achieve, and the brittleness of the PLA would make it difficult to cut the material without breaking it. Due to the time limit of the project it was decided to proceed with the injection molding despite the issues, but in retrospect choosing another method from start for preparing the specimen should probably have been more efficient.

It is also worth remembering that the characteristics of an injected molded specimen are not directly comparable to a 3D printed product. The injection molding subjects the material to higher shear rates and high pressures which affect the produced test specimen[41]. The characteristics of extruded materials are more similar to printed samples, which is why the characterizations in this project to the largest extent possible were executed on extruded material.

4.3 Differential scanning calorimetry

The heating DSC thermograms for each compound, obtained from the second temperature cycle at a heating rate of 10°C/min, are presented in Figure 4.3.

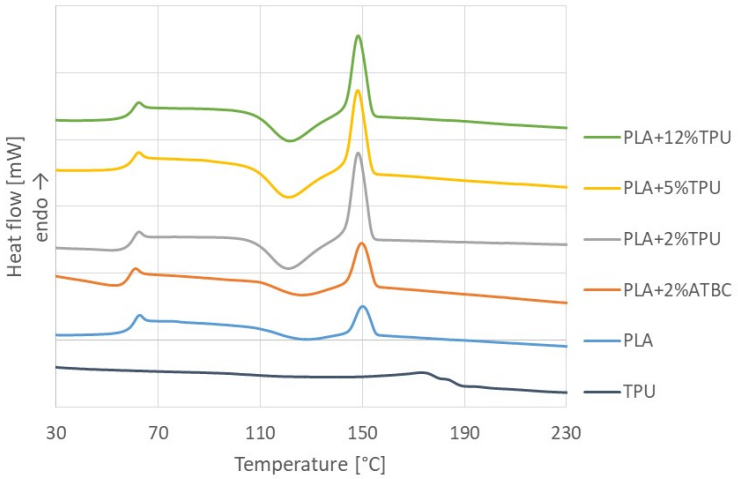

Figure 4.3: The heating DSC thermograms obtained from the second cycle at a heating rate of 10°C/min.

The transition temperatures identified from the heating of the second cycle are presented in Table 4.1. The T_g of pure TPU is below the investigated temperature range which is why a T_g of pure TPU is not observed. The other compounds exhibit a T_g around 58°C. Only one melting peak around 150°C is seen for each compound. Pure TPU has a melting peak around 170°C. The crystallinity of the compounds was calculated by investigating the area of the melting peaks. The degree of crystallinity, χ_c, is also presented in Table 4.1. The crystallinity of pure PLA is 1.1%, whereas the crystallinity of PLA+2%ATBC is 1.7% and the crystallinity of the TPU containing compounds is around 3%.

Table 4.1: The transition temperatures identified from the heating DSC thermograms from the second cycle at a heating rate of 10°C/min.

Compound	T_g [°C]	T_m [°C]	χ_c [%]
TPU	-	173.3	-
PLA	59.0	150.2	1.1
PLA+2%ATBC	57.6	149.8	1.7
PLA+2%TPU	58.8	148.3	3.5
PLA+5%TPU	58.5	148.1	3.1
PLA+12%TPU	58.7	148.5	3.0

The similarity in T_g means that the additives did not affect the T_g of PLA, which is desired for the intended application. There is a negligible difference in T_g between

pure PLA and PLA+2%ATBC, but it was expected that the addition of ATBC would decrease the T_g since that is a consequence of the addition of a plasticizer. The absence of a reduction of T_g might be due to 1. too low content of ATBC in the compound, 2. immiscibility of the plasticizer and the matrix, or 3. evaporation/migration of plasticizer during drying. A miscibility investigation is needed to excluded that the lack of a reduced T_g is due to the additive not being miscible in the polymer matrix.

The melting peak observed for the compounds is assigned to the melting of PLA. This melting peak of pure TPU is not observed for the compounds, which possibly could be explained by TPU not crystallizing in the blends or by TPU gradually melting together with the PLA crystals so that no separate melting peak is observed at 170°C. The melting temperature of the compounds containing TPU is slightly lower compared to pure PLA. Smaller crystals melts at lower temperatures than larger crystals due to the increased interfacial free energy in the smaller crystallites[15]. It is therefore possible that the observed decrease occurs because the added TPU interfere with the crystal growth of PLA, resulting in smaller or thinner crystals.

Evaluating the crystallinity of the compounds it can be concluded that at least the compounds containing TPU have a higher degree of crystallinity than pure PLA. This indicates that the TPU affects the crystallization of PLA, possibly by acting as a nucleating agent.

When using a lower heating rate (5°C/min) the transition temperatures are shifted to slightly lower values, in accordance with what is reported in literature[15]. It can also be observed in Figure 4.4, which shows the heating DSC thermograms from the second cycle at a heating rate of 5°C/min, that two melting peaks occur for the compounds containing TPU. This also indicates that TPU affects the crystallization of PLA, and gives rise to the presence of several crystalline phases of PLA which melts at different temperatures[19].

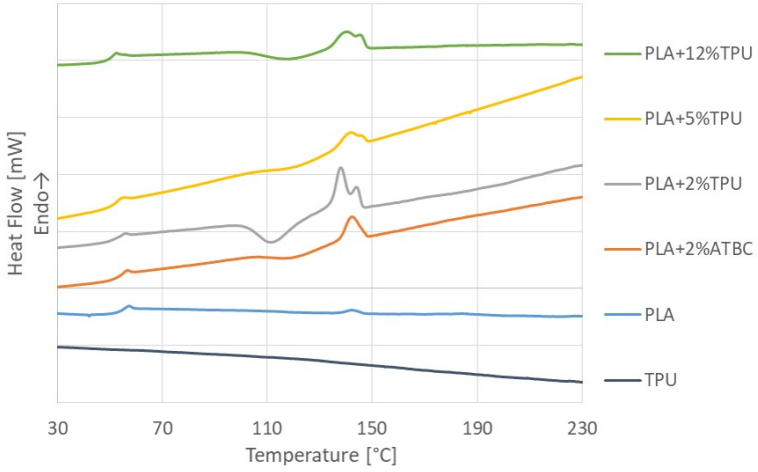

Figure 4.4: The heating DSC thermograms obtained from the second cycle at a heating rate of 5°C/min.

4.4 Capillary viscometry

The apparent viscosity as a function of shear rate for all compounds is presented in Figure 4.5. The apparent viscosity means that no corrections for pressure losses etc. have been calculated. The apparent viscosity of each compound is presented as a mean value of two measurements.

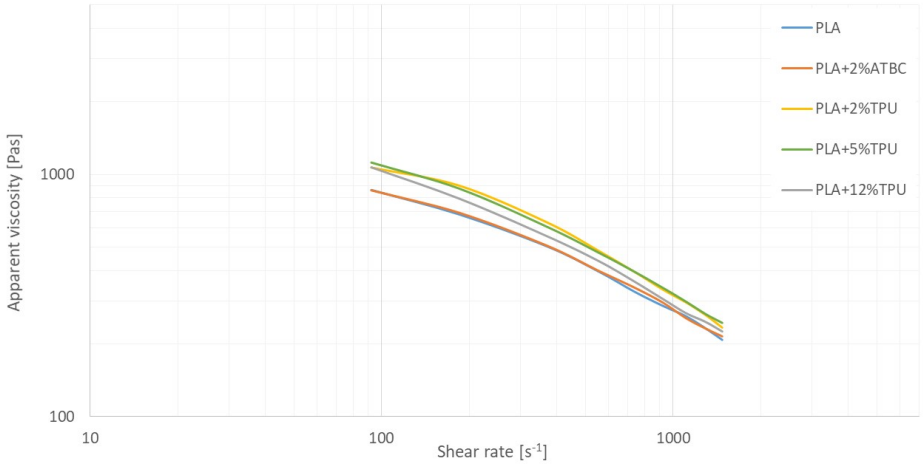

Figure 4.5: The apparent viscosity as a function of shear rate.

The viscosity of pure PLA ranges from 860 to 210 Pas exhibiting a shear thinning effect. The viscosity of PLA+2%ATBC shows the same behavior as pure PLA, also ranging from 860 to 210 Pas. The viscosity of PLA+2%ATBC slightly increases compared to pure PLA when the shear rate reaches above 600 s^{-1} but as the viscosity reaches 1000 s^{-1} the compounds show similar viscosity again.

The compounds containing TPU show higher viscosity than pure PLA. PLA+2%TPU and PLA+5%TPU exhibit very similar viscosity. The viscosity of PLA+2%TPU and PLA+5%TPU ranges from 1070 Pas to 230 Pas respectively 1120 Pas to 240 Pas. At shear rates under 100 s^{-1} PLA+2%TPU exhibits slightly lower viscosity and between 180 and 550 s^{-1} PLA+2%TPU exhibits slightly higher viscosity than PLA+5%TPU, whereas above 550 s^{-1} the viscosity of the two compounds is nearly identical. The viscosity of PLA+12%TPU also ranges from 1070 Pas to 230 Pas, but in-between the lowest and highest shear rates the viscosity of PLA+12%TPU is lower than for the two other TPU containing compounds.

The shear thinning behavior of pure PLA as well as the values of the viscosity are similar to what is found in literature[45]. This confirms the results for pure PLA obtained in this project. It was expected that the ATBC would decrease the viscosity since a plasticizer facilitates the movement of the polymer chains. A study showed that the addition of 5% ATBC increased the melt flow index of PLA with approximately 50%[28], which corresponds to a decrease in viscosity. The fact that no apparent decrease in viscosity is seen in this case might be due to the low plasticizer content in the material.

Regarding the viscosity of PLA-TPU compounds the theories found in literature differs. One study has reported that the viscosity of PLA-TPU compounds is an additive property, meaning that as the TPU content of the compound increases, the viscosity will change from being similar to pure PLA to become more similar to the viscosity of pure TPU[48]. Another study reported that with low TPU content (10-30%) the viscosity was lower than pure PLA due to the plasticizing effect of TPU while with higher TPU content (40-50%) the viscosity was higher than pure PLA because of increased interactions between PLA and TPU[33].

Neither of the results reported in these studies are in accordance with the obtained results in this project. The results found in literature and the results obtained in this project can differ because different types of PLA and TPU and different compositions of the compounds have been investigated. It can also be that the viscosity of PLA-TPU blends is a complex matter whose origin is not fully understood. In this project, only two measurements were conducted for each compound, so it is possible that more measurements and further investigations are needed to verify the results and to fully understand the melt flow behavior of these compounds.

The temperature, capillary diameter and shear rate that were used for the measurement were chosen to in a way mimic the extrusion of the filament in a 3D printer, and the desire was to keep the viscosity of the compounds containing additives the same as for PLA. Even if the viscosity of the compounds is slightly different, the difference in viscosity between the compounds decreases as the shear rate increases and the viscosity of all the materials are in the same region and follow the same trend as the pure PLA. This means that all the compounds are, with respect to their viscosity, suitable filaments for 3D printing. To what extent the small difference in viscosity of the TPU containing compounds affects the 3D printing process can only be determined by producing filaments of these compounds and investigating their behavior in a 3D printer.

4.5 Impact test

The impact strength of the compounds is presented in Figure 4.6. The impact strength, which is a mean of five measurements for each compound, is presented together with the standard deviation as error bars. The exact values of the impact strength and standard deviation are presented in Table 4.2.

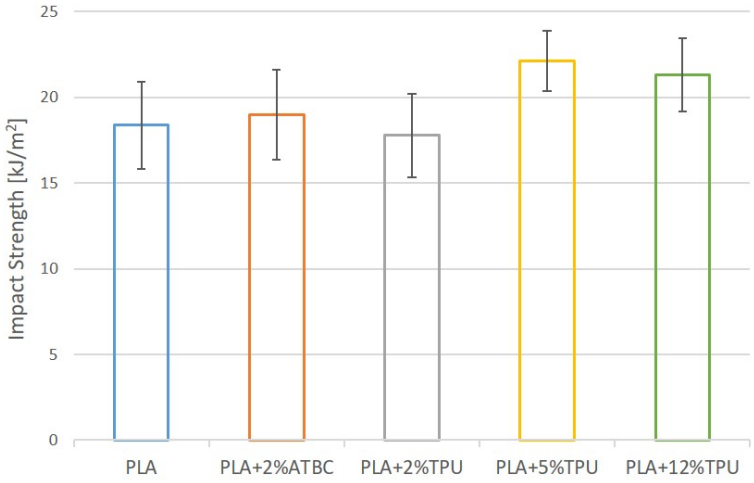

Figure 4.6: The impact strength of the compounds.

Pure PLA exhibits an impact strength of 18.4 kJ/m^2. Adding 2% ATBC increased the impact strength to 19.0 kJ/m^2 while the addition of 2% TPU decreased it to 17.8 kJ/m^2. This compound resulted in the lowest impact strength. PLA+5%TPU exhibits the highest impact strength at 22.1 kJ/m^2 while PLA+12%TPU resulted in an impact strength of 21.3 kJ/m^2.

Table 4.2: The impact strength for each compound and the corresponding standard deviation.

Compound	Impact Strength [kJ/m^2]	Std [kJ/m^2]
PLA	18.4	2.6
PLA+2%ATBC	19.0	2.6
PLA+2%TPU	17.8	2.4
PLA+5%TPU	22.1	1.8
PLA+12%TPU	21.3	2.1

The addition of ATBC slightly increased the impact strength compared to pure PLA, probably due to the plasticizing effect of ATBC. However, the standard deviations for PLA and PLA+2% ATBC are both 2.6 kJ/m^2 and their impact strength is quite

similar which means that the impact strength of these two compounds varies within the same range. The impact strength resulting from the addition of TPU does not show a clear trend. It is known that the addition of rubber can turn brittle polymers into high-impact materials[17], which why the decrease in impact strength by the addition of 2% TPU raises some questions. The decrease is however very small and considering the standard deviation it is not certain that the impact strength of PLA+2%TPU in fact is lower than pure PLA.

The impact strength of the compounds containing TPU exhibits an optimum at 5% TPU. It has been shown that the addition of rubber can increase the impact strength up to a certain limit, which depends on the morphology of the rubber phase[17]. If the rubber is dispersed in the polymer matrix as spherical particles the impact strength is often increased, but as the rubber content increases, the particle shape can change from spherical to elongated agglomerates[17]. When this transition is reached the impact strength has also reached its maximum[17]. It is possible that this transition is what is seen in this project when increasing the TPU content from 5% to 12% and therefore the compound containing 12% TPU exhibits a lower impact strength than PLA+5%TPU. The morphology of the compounds must nevertheless be investigated to confirm this theory.

Since the specimens were un-notched, two mechanisms are required for fracture; crack initiation and crack propagation[17]. These mechanisms are complex and to a great extent affected by internal stresses, voids or other defects in the specimens[17]. It is therefore possible that the shrinkage or other imperfection resulting from the injection molding is effecting the result. To limit the effect of these imperfections, more specimens could have been tested to obtain a more statistically reliable result.

For practical reasons, the edges of the injection molded specimens were not cut off prior to impact testing, which is not according to the ISO standard. It is possible that the edges of the specimens absorbed some energy from the pendulum which gave rise to the impression that the compounds possesses a higher impact strength than they actually do. Since the specimens for all compounds had the same shape this possible overestimation of the impact strength should be similar for all compounds and should therefore not affect the interpretation of the result.

4.6 Tensile test

The stress-strain curves obtained from the tensile test is presented in Figure A.1 in Appendix A. From these curves the yield stress and yield strain are obtained, presented in Figure 4.7. The values presented are a mean of five measurements per compound and the standard deviation is presented as error bars. All compounds exhibit similar yield stress, pure PLA and PLA+2%TPU exhibiting the most equal stresses. A small reduction is observed for PLA+2%ATBC and as the amount of TPU increases the yield stress of these compounds decreases.

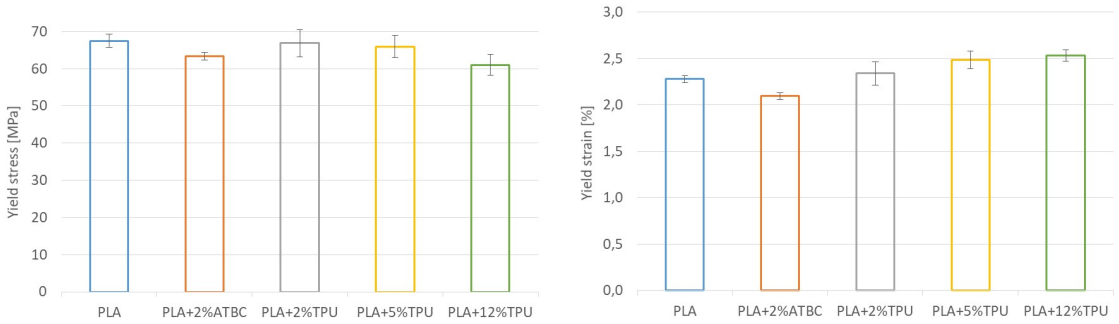

(a) Yield stress

(b) Yield strain

Figure 4.7: a) The yield stress and b) yield strain obtained from the tensile test.

The yield strain is almost the same for every compound, around 2%. Compared to pure PLA a small reduction is seen for PLA+2%ATBC and a small increase is observed for PLA+5%TPU and PLA+12%TPU. The exact values of the yield stress and yield strain, as well as the standard deviations, are presented in Table 4.3.

Table 4.3: The yield stress and yield strain for each compound and the corresponding standard deviations.

Compound	Yield stress [MPa]	Std [MPa]	Yield strain [%]	Std [%]
PLA	67.5	1.8	2.3	0.04
PLA+2%ATBC	63.4	1.0	2.1	0.04
PLA+2%TPU	66.9	3.7	2.3	0.13
PLA+5%TPU	66.0	2.9	2.5	0.09
PLA+12%TPU	61.0	2.8	2.5	0.06

The strain at break, or elongation at break, and Young's modulus are also obtained from the stress-strain curves. These values, as a mean of five measurements, are presented in Figure 4.8. Pure PLA, PLA+2%ATBC and PLA+2%TPU exhibit similar strain at break; 3.4%, 4.2% and 3.6%. The strain at break is clearly increased by the addition of 5% and 12% TPU, up to 92.9% and 197.1%. The standard deviation, presented as error bars in the graphs, shows that the measurements of PLA+5%TPU varies, but all measurements indicate that the strain at break is increased compared to pure PLA.

Young's modulus, or the elastic modulus, is higher for pure PLA than for the compounds containing additives, regardless of what additive present. Furthermore, the more TPU is added the more is the modulus reduced.

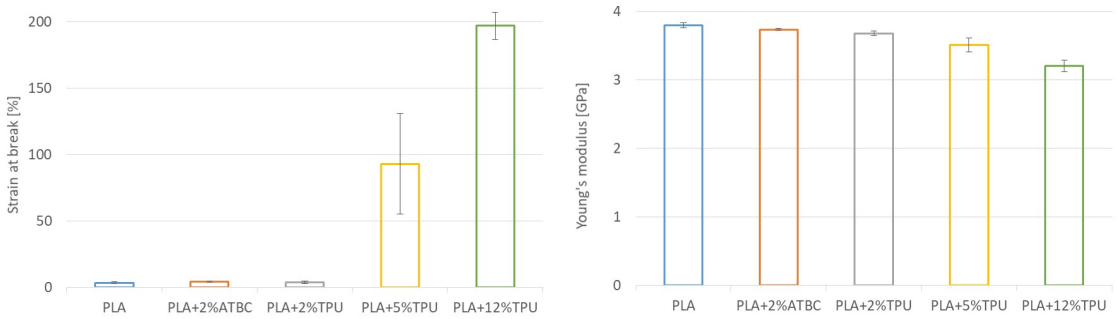

(a) Strain at break

(b) Young's modulus

Figure 4.8: a) The strain at break and b) Young's modulus obtained from the tensile test.

The exact values of the strain at break and Young's modulus, as well as the standard deviations, are presented in Table 4.4.

Table 4.4: The strain at break and Young's modulus for each compound and the corresponding standard deviations.

Compound	Strain at break [%]	Std [%]	Young's modulus [GPa]	Std [GPa]
PLA	3.4	0.6	3.8	0.04
PLA+2%ATBC	4.2	0.5	3.7	0.02
PLA+2%TPU	3.6	1.0	3.7	0.03
PLA+5%TPU	92.9	37.8	3.5	0.10
PLA+12%TPU	197.0	10.2	3.2	0.08

The results presented so far is from the so called engineering stress-strain curves. This means that the initial cross section of the specimens is used to calculate the stress. If the specimen exhibits necking the cross section is reduced as the specimen is elongated, so to account for this reduction of the cross section the so called true stress can be calculated. This was done by assuming a constant volume of the thinner part of the test specimen, and by knowing the extension of the test specimen in each recorded data point, a new cross section in each data point was calculated. This new cross section was then used to calculate the true stress. This is an approximate method, but it gives an indication of how the strength changes during the plastic deformation.

The engineering stress at break and the true stress at break, or ultimate tensile strength, are presented in Figure 4.9. The engineering stress at break shows no evident trend, except that the stress is reduced for all compounds compared to pure PLA. The standard deviation for PLA+2%TPU is very large, indicating a large variation of the measured specimens.

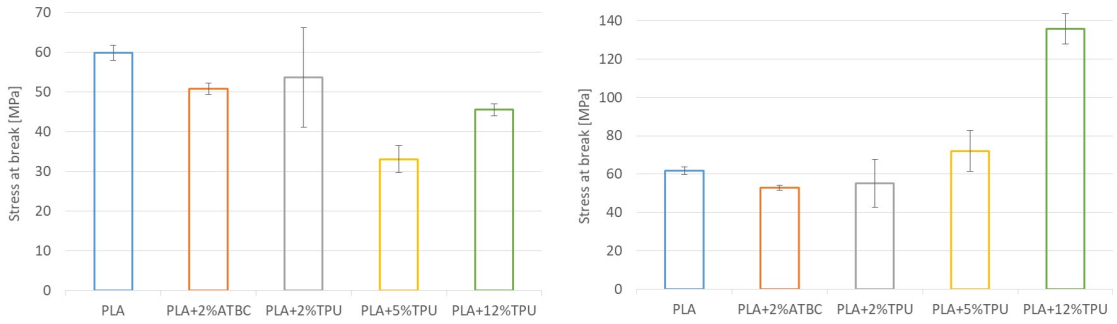

(a) Engineering stress at break

(b) True stress at break

Figure 4.9: a) The stress at break obtained from the engineering stress-strain diagram and b) the stress at break obtained from the true stress-strain diagram.

When instead evaluating the true stress at break, a clear trend of increasing stress at break is observed for PLA+5%TPU and PLA+12%TPU while PLA+2%ATBC and PLA+2%TPU exhibit slightly lower stress at break than pure PLA. The standard deviation is higher for the TPU containing additives than for pure PLA and PLA+2%ATBC. The exact values of the engineering stress at break and the true stress at break, as well as the standard deviation, are presented in Table 4.5.

Table 4.5: The engineering stress at break and the true stress at break for each compound and the corresponding standard deviations.

Compound	Eng. stress at break [MPa]	Std [MPa]	True stress at break [%]	Std [MPa]
PLA	59.8	2.0	61.9	2.0
PLA+2%ATBC	50.8	1.4	53.0	1.3
PLA+2%TPU	53.6	12.5	55.3	12.5
PLA+5%TPU	33.0	3.4	72.1	10.8
PLA+12%TPU	45.5	1.5	135.7	8.0

The reason behind the resulting engineering stress at break is not clear. All compounds containing additives exhibit a lower stress at break than pure PLA, but no evident trend is observed. As for the impact test, it is possible that internal stresses or defects in the specimens resulting from the injection molding affect the fracturing of the specimens. However, the true stress at break is more accurate when studying ductile materials. From the true stress at break, the strain hardening resulting from the plastic deformation of PLA+5%TPU and PLA+12%TPU is clearly observed.

Since PLA+2%ATBC and PLA+2%TPU have not affected the mechanical properties of PLA significantly, it is possible that 2% of is not enough, regardless of additive, to induce the desired changes. PLA+2%ATBC has throughout the project showed very small differences from pure PLA, which is why an investigation of the morphology and the miscibility would be helpful to fully understand the reason behind the results. The addition of 5% and 12% TPU instead indicates an increased

ductility of PLA by the increase of the elongation at break, which is assigned to the elastic properties of TPU. The reduction of Young's modulus also indicates that these compounds lose their stiffness and becomes more elastic compared to pure PLA.

4.7 Sources of error

It is possible that injection molding the specimens for the mechanical tests brought some uncertainty to the results. The injection molding was a very troublesome process, and even though the optimization was carefully executed some shrinkage along the test specimens and the manual loading of shot volume was not possible to avoid.

To what extent these issues affected the impact and tensile tests is hard to tell. An attempt to reduce the effects of the shrinkage was made by for example measuring the shrinkage when calculating the cross sections of the specimens. However, choosing another method, for example compression molding or 3D printing, for the preparation of the test specimen could possibly eliminate the defects that occurred from the injection molding.

5
Future Work

The miscibility and the morphology of the compounds need to be investigated to gain a deeper understanding of the properties of the compounds. It is also of great importance when commercializing a compound as a 3D printing filament that the life time of the filament if sufficient. The physical aging of the compounds is therefore important to investigate, which depends on the miscibility of the additive and the polymer matrix. Therefore, FTIR and SEM could be complementary analyses to this project. FTIR can be used to detect any chemical bonds between the additive and the polymer matrix and SEM can be used to investigate how the additive is dispersed in the matrix.

The viscosity of the TPU containing compounds is not fully understood. In addition to studying the morphology of the compounds, conducting additional viscosity measurements could also be valuable in order to verify that the obtained results are reliable.

The addition of 2% gave a relatively small impact on the thermal as well as the mechanical properties of the compound. If it is concluded that ATBC and PLA is not immiscible, it would be of interest to study the effect of a larger addition of this plasticizer.

To further understand the properties of the compounds, TGA could be used to investigate how the additives affect the thermal stability of PLA and a more in-depth analysis of the crystallinity of the compounds could be conducted using XRD. An investigation of how to increase the heat resistance of PLA was not included in this project, but can be of importance to further enhance the properties of PLA. It would also be interesting to investigate if a reduced brittleness can be combined with an increased heat resistance by preparing a compound that contains a plasticizer together with a fiber or some kind of reinforcement.

The final investigation of how well these compounds would perform as 3D printing filaments would be to prepare filaments from these compounds and investigate the printing process in a 3D printer.

6
Conclusion

In this project, five different compounds (PLA, PLA+2%ATBC, PLA+2%TPU, PLA+5%TPU and PLA+12%TPU) have been prepared and their thermal and mechanical properties have been characterized in order to find suitable PLA compounds with enhanced properties for the use as 3D printing filament. From the preparation of the compounds it can be concluded that investigated materials are difficult to process, leading to problems with extrusion as well as injection molding.

The characterization of the compounds showed that all compounds have transition temperatures similar to pure PLA and suitable viscosity at the shear rates used in 3D printing. With respect to the transition temperatures and the viscosity, all the compounds are potentially suitable filaments for 3D printing.

The impact test showed that the addition of 5% and 12% TPU increased the impact strength, PLA+5%TPU exhibiting the highest strength. The addition of 2% ATBC and 2% TPU did not change the impact strength of PLA significantly. The tensile test showed that the addition of 5% and 12% TPU increased the elongation at break and decreased Young's modulus, 12% TPU exhibiting the largest change compared to pure PLA. This indicates that these compounds are more ductile than pure PLA. These two compounds also exhibited the largest reduction of the engineering stress at break, but when studying the true stress at break, the strain hardening of these compounds was evident.

The addition of 2% ATBC and 2% TPU did not change the mechanical properties obtained from the tensile test to a large extent. Is has been concluded from several characterization methods that the addition of 2% ATBC possibly is an insufficient amount of this particular additive to influence the properties of PLA.

When summarizing all the results obtained in this project, PLA+5%TPU and PLA+12%TPU are the compounds, that in addition to suitable transition temperatures and viscosity, also show enhanced mechanical properties. PLA+5%TPU and PLA+12%TPU are therefore the compounds that could be most suitable to use as 3D printing filaments. Additional investigations of the compounds are however necessary to verify the results and to further understand their properties.

Bibliography

[1] Å. Stenmarck *et al.*, "Ökad plaståtervinning – potential för utvalda produktgrupper," *Naturvårdsverket*, 2018. [Online]. Available: https://www.naturvardsverket.se/Documents/publikationer6400/978-91-620-6844-8.pdf?pid=23338

[2] X. Wang, M. Jiang, Z. Zhou, J. Gou, and D. Hui, "3D Printing of Polymer Matrix Composites: A Review and Prospective," *Composites Part B: Engineering*, vol. 110, pp. 442 – 458, 2017, doi:10.1016/j.compositesb.2016.11.034. [Online]. Available: http://www.sciencedirect.com/science/article/pii/S1359836816321230

[3] W. Liu, J. Zhou, Y. Ma, J. Wang, and J. Xu, "Fabrication of PLA Filaments and its Printable Performance," *IOP Conference Series: Materials Science and Engineering*, vol. 275, pp. 12–33, 2017, doi:10.1088/1757-899x/275/1/012033. [Online]. Available: https://iopscience.iop.org/article/10.1088/1757-899X/275/1/012033

[4] J. Slapnik, R. Bobovnik, M. Mešl, and S. Bolka, "Modified Polylactide Filaments for 3D Printing with Improved Mechanical Properties," *Contemporary Materials*, vol. 2, no. 7, pp. 142–150, 2016, doi:10.7251/COMEN1602142S. [Online]. Available: http://savremenimaterijali.info/sajt/doc/file/casopisi/7_2/7-Slapnik.pdf

[5] K. A. Afrifah and L. M. Matuana, "Impact Modification of Polylactide with a Biodegradable Ethylene/Acrylate Copolymer," *Macromolecular Materials and Engineering*, vol. 295, no. 9, pp. 802–811, 2010, doi:10.1002/mame.201000107. [Online]. Available: https://onlinelibrary.wiley.com/doi/full/10.1002/mame.201000107

[6] R. P. Singh and D. W. Kent-Jones, "Cereal processing," *Encyclopædia Britannica, inc.*, 2010. [Online]. Available: https://www.britannica.com/technology/cereal-processing

[7] T. Yamane, "Sugarcane," *Encyclopædia Britannica, inc.*, 2018. [Online]. Available: https://www.britannica.com/plant/sugarcane

[8] J. M. Ferri, D. Garcia-Garcia, N. Montanes, O. Fenollar, and R. Balart, "The Effect of Maleinized Linseed Oil as Biobased Plasticizer in Poly(lactic acid)-based Formulations," *Polymer International*, vol. 66, no. 6, pp. 882–891, 2017, doi:10.1002/pi.5329. [Online]. Available: https://onlinelibrary.wiley.com/doi/abs/10.1002/pi.5329

[9] "Overview of materials for Acrylonitrile Butadiene Styrene (ABS), Extruded," Matweb.com, Accessed: 2019-02-04. [Online]. Available: http://www.matweb.

com/search/DataSheet.aspx?MatGUID=3a8afcddac864d4b8f58d40570d2e5aa

[10] "Acrylonitrile Butadiene Styrene (ABS)," Makeitfrom.com, Accessed: 2019-02-04. [Online]. Available: https://www.makeitfrom.com/material-properties/Acrylonitrile-Butadiene-Styrene-ABS

[11] "Overview of materials for Polylactic Acid (PLA) Biopolymer," Matweb.com, Accessed: 2019-02-04. [Online]. Available: http://www.matweb.com/search/DataSheet.aspx?MatGUID=ab96a4c0655c4018a8785ac4031b9278&ckck=1

[12] "Polylactic Acid (PLA, Polylactide)," Makeitfrom.com, Accessed: 2019-02-04. [Online]. Available: https://www.makeitfrom.com/material-properties/Polylactic-Acid-PLA-Polylactide

[13] S. Wang, L. Capoen, D. R. D'hooge, and L. Cardon, "Can the melt flow index be used to predict the success of fused deposition modelling of commercial poly(lactic acid) filaments into 3d printed materials?" *Plastics, Rubber and Composites*, vol. 47, no. 1, pp. 9–16, 2018, doi:10.1080/14658011.2017.1397308. [Online]. Available: https://www.tandfonline.com/doi/full/10.1080/14658011.2017.1397308?scroll=top&needAccess=true

[14] G. Xie, Y. Zhang, and W. Lin, "Plasticizer Combinations and Performance of Wood Flour–Poly(Lactic Acid) 3D Printing Filaments," *BioResources*, vol. 12, no. 3, pp. 6736–6748, 2017. [Online]. Available: http://stargate.cnr.ncsu.edu/index.php/BioRes/article/view/BioRes_12_3_6736_Xie_Plasticizer_Performance_Printing_Filaments

[15] J. M. G. Cowie and V. Arrighi, *Polymers: Chemistry and Physics of Modern Materials*. Chapman and Hall/CRC, 2007. [Online]. Available: https://ebookcentral.proquest.com/lib/chalmers/detail.action?docID=1449424

[16] N. Peelman *et al.*, "Heat resistance of new biobased polymeric materials, focusing on starch, cellulose, PLA, and PHA," *Journal of Applied Polymer Science*, vol. 132, no. 48, 2015, doi:10.1002/app.42305. [Online]. Available: https://onlinelibrary.wiley.com/doi/abs/10.1002/app.42305

[17] L. E. Nielsen and R. F. Landel., *Mechanical Properties of Polymers and Composites*. CRC Press, 1994.

[18] B. Gupta, N. Revagade, and J. Hilborn, "Poly(lactic acid) fiber: An overview," *Progress in Polymer Science*, vol. 32, no. 4, pp. 455 – 482, 2007, doi:10.1016/j.progpolymsci.2007.01.005. [Online]. Available: http://www.sciencedirect.com/science/article/pii/S007967000700007X

[19] S. Saeidlou, M. A. Huneault, H. Li, and C. B. Park, "Poly(lactic acid) crystallization," *Progress in Polymer Science*, vol. 37, no. 12, pp. 1657 – 1677, 2012, doi:/10.1016/j.progpolymsci.2012.07.005. [Online]. Available: http://www.sciencedirect.com/science/article/pii/S0079670012000792

[20] T. Tábi, I. Sajó, F. Szabó, A. Luyt, and J. Kovács, "Crystalline structure of annealed polylactic acid and its relation to processing," *Express Polymer Letters*, vol. 4, no. 10, 2010, doi:10.3144/expresspolymlett.2010.80. [Online]. Available: http://www.expresspolymlett.com/articles/EPL-0001596_article.pdf

[21] "Crystallizing and Drying Inego Biopolymer," NatureWorks, n.d, Accessed: 2019-04-09. [Online]. Available: https://www.natureworksllc.

com/~/media/Files/NatureWorks/Technical-Documents/Processing-Guides/ProcessingGuide_Crystallizing-and-Drying_pdf.pdf?la=en

[22] L. H. Sperling, *Introduction to Physical Polymer Science*. Wiley, 2006. [Online]. Available: http://proxy.lib.chalmers.se/login?url=http://search.ebscohost.com/login.aspx?direct=true&db=cat06296a&AN=clc.b1333704&site=eds-live&scope=site

[23] B. W. Chieng, N. A. Ibrahim, Y. Y. Then, and Y. Y. Loo, "Epoxidized Vegetable Oils Plasticized Poly(lactic acid) Biocomposites: Mechanical, Thermal and Morphology Properties," *Molecules*, vol. 19, no. 10, pp. 16 024–16 038, 2014, doi:10.3390/molecules191016024. [Online]. Available: http://www.mdpi.com/1420-3049/19/10/16024

[24] M. Wang, Y. Wu, Y.-D. Li, and J.-B. Zeng, "Progress in Toughening Poly(Lactic Acid) with Renewable Polymers," *Polymer Reviews*, vol. 57, no. 4, pp. 557–593, 2017, doi:10.1080/15583724.2017.1287726. [Online]. Available: https://www.tandfonline.com/doi/abs/10.1080/15583724.2017.1287726

[25] Experimental investigations conducted by C.Johansson, Chalmers Industriteknik, within the project lead by Add North, spring 2018.

[26] I. Harte, C. Birkinshaw, E. Jones, J. Kennedy, and E. DeBarra, "The effect of citrate ester plasticizers on the thermal and mechanical properties of poly(DL-lactide)," *Journal of Applied Polymer Science*, vol. 127, no. 3, pp. 1997–2003, 2013, doi:10.1002/app.37600. [Online]. Available: https://onlinelibrary.wiley.com/doi/abs/10.1002/app.37600

[27] P. Menčík *et al.*, "Effect of Selected Commercial Plasticizers on Mechanical, Thermal, and Morphological Properties of Poly(3-hydroxybutyrate)/Poly(lactic acid)/Plasticizer Biodegradable Blends for Three-Dimensional (3D) Print," *Materials*, vol. 11, no. 10, 2018, doi:10.3390/ma11101893. [Online]. Available: http://www.mdpi.com/1996-1944/11/10/1893

[28] M. Maiza, M. T. Benaniba, G. Quintard, and V. Massardier-Nageotte, "Biobased additive plasticizing Polylactic acid (PLA)," *Polimeros*, vol. 25, pp. 581 – 590, 2015, doi:10.1590/0104-1428.1986. [Online]. Available: http://www.scielo.br/scielo.php?script=sci_arttext&pid=S0104-14282015000600581&nrm=iso

[29] M. Khemakhem, K. Lamnawar, A. Maazouz, and M. Jaziri, "Effect of core–shell acrylate rubber particles on the thermomechanical and physical properties of biocomposites from polylactic acid and olive solid waste," *Polymer Engineering & Science*, vol. 58, no. 6, pp. 894–902, 2018, doi:10.1002/pen.24642. [Online]. Available: https://onlinelibrary.wiley.com/doi/abs/10.1002/pen.24642

[30] T. Li, L.-S. Turng, S. Gong, and K. Erlacher, "Polylactide, nanoclay, and core–shell rubber composites," *Polymer Engineering & Science*, vol. 46, no. 10, pp. 1419–1427, 2006, doi.:10.1002/pen.20629. [Online]. Available: https://onlinelibrary.wiley.com/doi/abs/10.1002/pen.20629

[31] P. Sookprasert and N. Hinchiranan, "Morphology, mechanical and thermal properties of poly(lactic acid) (PLA)/natural rubber (NR) blends compatibilized by NR-graft-PLA," *Journal of Materials Research*, vol. 32, no. 4, p. 788–800, 2017, doi:10.1557/jmr.2017.9. [Online]. Available: https://www.cambridge.org/core/services/aop-cambridge-core/content/

view/FA1578EEB46F7C549C6E16AC9D2486DB/S0884291417000097a.pdf/morphology_mechanical_and_thermal_properties_of_polylactic_acid_planatural_rubber_nr_blends_compatibilized_by_nrgraftpla.pdf

[32] F. Feng and L. Ye, "Morphologies and Mechanical Properties of Polylactide/Thermoplastic Polyurethane Elastomer Blends," *Journal of Applied Polymer Science*, vol. 119, no. 5, pp. 2778–2783, 2011, doi:10.1002/app.32863. [Online]. Available: https://onlinelibrary.wiley.com/doi/abs/10.1002/app.32863

[33] H. Hong *et al.*, "A novel composite coupled hardness with flexibleness—polylactic acid toughen with thermoplastic polyurethane," *Journal of Applied Polymer Science*, vol. 121, no. 2, pp. 855–861, 2011, doi:10.1002/app.33675. [Online]. Available: https://onlinelibrary.wiley.com/doi/abs/10.1002/app.33675

[34] Telephone communication with E.Bengtsson, Add North. 2019-02-06.

[35] Y. Wang, S. M. Chiao, T.-F. Hung, and S.-Y. Yang, "Improvement in toughness and heat resistance of poly(lactic acid)/polycarbonate blend through twin-screw blending: Influence of compatibilizer type," *Journal of Applied Polymer Science*, vol. 125, no. S2, pp. E402–E412, 2012, doi:10.1002/app.36920. [Online]. Available: https://onlinelibrary.wiley.com/doi/abs/10.1002/app.36920

[36] C. Benwood, A. Anstey, J. Andrzejewski, M. Misra, and A. K. Mohanty, "Improving the Impact Strength and Heat Resistance of 3D Printed Models: Structure, Property, and Processing Correlationships during Fused Deposition Modeling (FDM) of Poly(Lactic Acid)," *ACS Omega*, vol. 3, no. 4, pp. 4400–4411, 2018, doi:10.1021/acsomega.8b00129. [Online]. Available: https://doi.org/10.1021/acsomega.8b00129

[37] N. A. Sukindar, M. K. A. Ariffin, B. T. Baharudin, C. N. A. Jaafar, and M. I. S. Ismail, "Analyzing the effect of nozzle diameter in fused deposition modeling for extruding polylactic acid using open source 3d printing," *Jurnal Teknologi*, vol. 78, no. 10, pp. 7–15, 2016, doi:10.11113/jt.v78.6265. [Online]. Available: http://www.diale.org/pdf/3DThesis/Analyzing_the_effect_of_nozzle_diameter_in_fused_d-1.pdf

[38] R. Chokshi and H. Zia, "Hot-Melt Extrusion Technique: A Review," *Iranian Journal of Pharmaceutical Research*, vol. 3, no. 1, pp. 3–16, 2010. [Online]. Available: http://ijpr.sbmu.ac.ir/article_290_799880c70748d24fb06fec28351e1577.pdf

[39] L.-S. Turng and S. H. Goodman, "Plastics Processing," *AccessScience, McGraw-Hill Education*, 2014, doi:10.1036/1097-8542.526800. [Online]. Available: https://www.accessscience.com/content/plastics-processing/526800#

[40] A. Naranjo, M. del Pilar Noriega, T. A. Osswald, A. Roldán-Alzate, and J. D. Sierra, "Melt Rheology," in *Plastics Testing and Characterization - Industrial Applications*. Hanser Publishers, 2008, pp. 127–184. [Online]. Available: https://app.knovel.com/hotlink/khtml/id:kt008VK3Q5/plastics-testing-characterization/capillary-viscometer

[41] "Practical: Rheology," Laboratory Manual, Department of Materials and Manufacturing Technology, Chalmers University of Technology.

[42] S. E. Hughes, "Non-destructive and Destructive Testing," in *A Quick Guide to Welding and Weld Inspection*. Woodhead Publishing, 2009,

pp. 67 – 87, doi:10.1016/B978-1-84569-641-2.50006-4. [Online]. Available: http://www.sciencedirect.com/science/article/pii/B9781845696412500064

[43] N. S. Stoloff, "Mechanical Properties of Metal," *AccessScience, McGraw-Hill Education*, 2014, doi:10.1036/1097-8542.417810. [Online]. Available: https://www.accessscience.com/content/417810#417810s012

[44] "Plastics - determination of charpy impact properties – part 1: Non-instrumented impact test," ISO 179-1:2010.

[45] M. Mihai and R. Gendron, "Extrusion Foaming of Polylactide," in *Polymeric Foams: Innovations in Processes, Technologies, and Products*. CRC Press Taylor Francis Group, 2016.

[46] M. Charlon *et al.*, "Synthesis, structure and properties of fully biobased thermoplastic polyurethanes, obtained from a diisocyanate based on modified dimer fatty acids, and different renewable diols," *European Polymer Journal*, vol. 61, pp. 197 – 205, 2014, doi:doi.org/10.1016/j.eurpolymj.2014.10.012. [Online]. Available: http://www.sciencedirect.com/science/article/pii/S0014305714003632

[47] H. Blache *et al.*, "New bio-based thermoplastic polyurethane elastomers from isosorbide and rapeseed oil derivatives," *Industrial Crops and Products*, vol. 121, pp. 303 – 312, 2018, doi:doi.org/10.1016/j.indcrop.2018.05.004. [Online]. Available: http://www.sciencedirect.com/science/article/pii/S0926669018304151

[48] V. Jašo, M. Cvetinov, S. Rakić, and Z. S. Petrović, "Bio-Plastics and Elastomers from Polylactic Acid/Thermoplastic Polyurethane Blends," *Journal of Applied Polymer Science*, vol. 131, no. 22, 2014, doi:10.1002/app.41104. [Online]. Available: https://onlinelibrary.wiley.com/doi/abs/10.1002/app.41104

A

Appendix 1

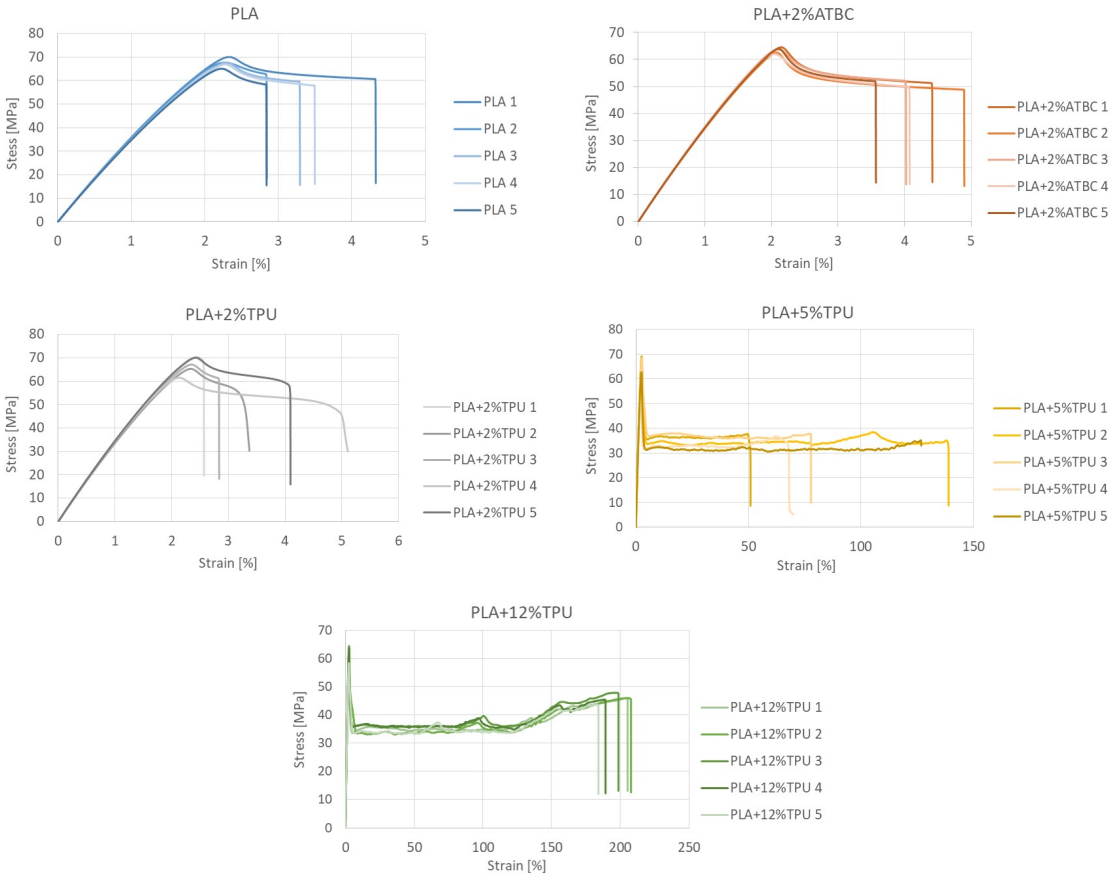

Figure A.1: The engineering stress-strain curves obtained from the tensile test.